

**RAINDROP ENERGY HARVESTING BASED ON STRETCHABLE  
ELECTRONIC**

**TIU KE XIN**

**A project report submitted in partial fulfilment of the requirements for the  
award of Master of Engineering (Electronic Systems)**

**Lee Kong Chian Faculty of Engineering and Science  
Universiti Tunku Abdul Rahman**

**May 2019**

**DECLARATION**

I hereby declare that this project report is based on my original work except for citations and quotations which have been duly acknowledged. I also declare that it has not been previously and concurrently submitted for any other degree or award at UTAR or other institutions.

Signature : \_\_\_\_\_

Name : TIU KE XIN  
\_\_\_\_\_

ID No. : 1805796  
\_\_\_\_\_

Date : \_\_\_\_\_

**APPROVAL FOR SUBMISSION**

I certify that this project report entitled “**RAINDROP ENERGY HARVESTING BASED ON STRETCHABLE ELECTRONIC**” was prepared by **TIU KE XIN** has met the required standard for submission in partial fulfilment of the requirements for the award of Master of Engineering (Electronics System) at Universiti Tunku Abdul Rahman.

Approved by,

Signature : \_\_\_\_\_

Supervisor : Dr. Chee Pei Song

Date : \_\_\_\_\_

The copyright of this report belongs to the author under the terms of the copyright Act 1987 as qualified by Intellectual Property Policy of Universiti Tunku Abdul Rahman. Due acknowledgement shall always be made of the use of any material contained in, or derived from, this report.

© 2019, Tiu Ke Xin. All right reserved.

## ACKNOWLEDGEMENTS

I would like to thank everyone who had contributed to the successful completion of this project. I would like to express my gratitude to my research supervisor, Dr. Chee Pei Song for his invaluable advice, guidance and his enormous patience throughout the development of the research.

In addition, I would also like to express my gratitude to my loving parents who had given me encouragement and support all the way and let me fully focus on my research project. I was felt thankful to my seniors and friends for their generous helps when I asked for it.

I also want to thank all the UTAR lab officer and assistants for their effort for providing the lab facilities and materials, as well as their services.

## ABSTRACT

To reduce depending on using battery for long term, energy harvesting method is always introduced in many areas by harvesting the energy from environment sources or human sources. In this project, the concept of electromagnetic energy harvesting is suggested to be self-power the device without using batteries. This concept will be applied in raindrop energy harvesting which is a process of generating the electricity by vibrating the stretchable prototype while the rain droplets fall on its surface. In practice, a stretchable prototype will be fabricated by using Ecoflex 0030 which has lower Young Modulus of about 69 kPa and is softer than PDMS, and applies conductive liquid such as EGaIn liquid or Galinstan to fill in the spiral coil. This research will more concentrate on Comsol multiphysics 5.3a to perform the simulation by moving the spiral coil in different direction to pass through the magnetic flux and thus produces electricity. All the model instructions have been illustrated clearly. Different characteristics such as the distance between Neodymium magnet and stretchable material, the quantity of magnets and so on will be studied to compare the better output that can power the electronic device. Future work and improvement are illustrated in the end as well.

## TABLE OF CONTENTS

<b>DECLARATION</b>	<b>ii</b>
<b>APPROVAL FOR SUBMISSION</b>	<b>iii</b>
<b>ACKNOWLEDGEMENTS</b>	<b>v</b>
<b>ABSTRACT</b>	<b>vi</b>
<b>TABLE OF CONTENTS</b>	<b>vii</b>
<b>LIST OF TABLES</b>	<b>x</b>
<b>LIST OF FIGURES</b>	<b>xii</b>
<b>LIST OF SYMBOLS / ABBREVIATIONS</b>	<b>xiii</b>

### CHAPTER

<b>1</b>	<b>INTRODUCTION</b>	<b>1</b>
	1.1 General Introduction	1
	1.2 Importance of the Study	2
	1.3 Problem Statement	2
	1.4 Aims and Objectives	3
	1.5 Scope and Limitation of the Study	3
	1.6 Outline of the Report	4
<b>2</b>	<b>LITERATURE REVIEW</b>	<b>5</b>
	2.1 Introduction	5
	2.2 Energy Harvesting	5
	2.2.1 Environmental Sources	6
	2.2.1.1 Solar Energy	6
	2.2.1.2 Infrared Radiator	7
	2.2.1.3 Wireless Energy Transfer	8
	2.2.1.3.1 Ultrasonic Energy Harvesting	8

	2.2.1.3.2	Inductive Energy Harvesting	9
	2.2.1.3.3	Capacitive Coupling Link	10
	2.2.2	Human Sources	11
	2.2.2.1	Thermal Energy	11
	2.2.2.2	Kinetic Energy	12
	2.2.2.2.1	Magnetic Induction Generator	13
	2.2.2.2.2	Electrostatic Energy	14
	2.2.2.2.3	Piezoelectricity	15
	2.3	Conductive Liquids	16
	2.4	Stretchable Material	18
	2.5	Spiral Coil	19
	2.6	Summary	20
<b>3</b>		<b>METHODOLOGY AND WORK PLAN</b>	<b>21</b>
	3.1	Introduction	21
	3.2	Brief Concept about Raindrop Energy Harvesting on Stretchable Electronic.	21
	3.3	Flowcharts for Modelling Instructions of the Simulations	23
	3.4	Modelling Instruction for Moving Coil in Vertical Direction with Two Fixed Neodymium Magnets	24
	3.5	Modelling Instruction for Moving Coil in Horizontal Direction with Two Fixed Neodymium Magnets	28
<b>4</b>		<b>RESULTS AND DISCUSSIONS</b>	<b>32</b>
	4.1	Introduction	32
	4.2	The Simulation of Spiral Coil Moving in Vertical Direction with One Fixed Permanent Magnet	32
	4.3	The Simulation of Spiral Coil Moving in Vertical Direction with Two Fixed Permanent Magnets	36
	4.4	The Simulation of Spiral Coil Moving in Horizontal Direction with Two Fixed Permanent Magnets	39
	4.5	Summary	41

<b>5</b>	<b>CONCLUSIONS AND RECOMMENDATIONS</b>	<b>42</b>
5.1	Conclusions	42
5.2	Recommendations for future work	44
	<b>REFERENCES</b>	<b>45</b>

## LIST OF TABLES

<b>TABLE</b>	<b>TITLE</b>	<b>PAGE</b>
<b>2.1</b>	The Parameters of Piezoelectricity.	<b>15</b>
<b>2.2</b>	Pros and Cons of Piezoelectricity.	<b>16</b>
<b>2.3</b>	The Comparison of Properties of Galinstan and Mercury.	<b>17</b>
<b>3.1</b>	The Parameters of Global Definition.	<b>24</b>
<b>3.2</b>	The Parameters of Geometry for Figure 3.2.	<b>25</b>
<b>3.3</b>	The Parameters for Prescribed Deformation.	<b>26</b>
<b>3.4</b>	The Material of Geometry for each Domain.	<b>26</b>
<b>3.5</b>	The Parameters of Global Definitions.	<b>28</b>
<b>3.6</b>	The Parameters of Geometry for Figure 3.3.	<b>28</b>
<b>3.7</b>	The Parameters for Prescribed Deformation.	<b>29</b>
<b>3.8</b>	The Material of Geometry for each Domain.	<b>30</b>
<b>4.1</b>	The Distance between one Magnet and Spiral Coil with 5.5 Turns with the respect of Output Peak Voltage.	<b>33</b>
<b>4.2</b>	The Distance between one Magnet and Spiral Coil with 10 turns with the respect of Output Peak Voltage.	<b>35</b>
<b>4.3</b>	The Distance between two Magnets and Spiral Coil with 5.5 turns with the respect of Output Peak Voltage.	<b>37</b>
<b>4.4</b>	The Distance between two Magnets and Spiral Coil with 10 Turns with the respect of Output Peak Voltage.	<b>38</b>
<b>4.5</b>	The Output Waveform when the Distance between Magnets and Stretchable Material is 0.8cm with the respect of Prescribed Deformation.	<b>40</b>
<b>4.6</b>	The Output Waveform when the Distance between Magnets and Stretchable Material is 0.3cm with the respect of Prescribed Deformation.	<b>41</b>

## LIST OF FIGURES

<b>FIGURE</b>	<b>TITLE</b>	<b>PAGE</b>
1.1	Dimension Scale of MEMS and Nanotechnology	1
2.1	Energy Harvesting Methods.	6
2.2	The Structure and the Operation of Solar Cell.	7
2.3	Wireless Energy System Powered by Infrared Radiation.	8
2.4	Ultrasonic Energy Harvesting Method with Implanted Device.	9
2.5	An Inductive Coupling Link System with Bidirectional Data Transmission.	10
2.6	The Simplified Capacitive Coupling Link.	11
2.7	The Equivalent Scheme of Thermoelectric Module with Thermopile.	12
2.8	Seebeck Effect of the Thermoelectric Module.	12
2.9	Magnetic Induction Generator with (a) Relative Motion and (b) Rigid Body Motion.	13
2.10	Seiko Wristwatch Using Seiko Kinetic Approach.	13
2.11	The Electrostatic Transducer under the Operation of Constant Charge and Constant Voltage.	14
2.12	Stretchable Electronic Surfaces with Different Values in Young Modulus.	18
2.13	Different Pattern of Coil Shape for Microchannel	19
3.1	Experimental Setup.	21
3.2	Stretchable Prototype in 2D Axial Symmetric Model where the Coil is moving in Vertical Direction.	22
3.3	Stretchable Prototype in 2D Axial Symmetric Model where the Coil is moving in Horizontal Direction.	22
3.4	The Flowchart for both Simulations.	23
4.1	The 2D and 3D Magnetic Flux Density Norm (T in unit) Created by One Magnet where Coil moves in Vertical Direction..	32
4.2	The 2D and 3D Magnetic Flux Density Norm (T in unit) Created by Two Magnets where Coil moves in Vertical Direction.	36
4.3	The 2D and 3D Magnetic Flux Density Norm (T in unit) Created by Two Magnets where Coil moves in Horizontal Direction.	39
5.1	The Comparison of Output Voltage for Each Characteristic When Coil is Moving in Vertical Direction.	43
5.2	The Comparison of Output Voltage for Each Characteristic When Coil is Moving in Horizontal Direction.	43
5.3	Different Types of Rectifying Circuit for Energy Storage	44

**LIST OF SYMBOLS / ABBREVIATIONS**

$c_p$	specific heat capacity, J/(kg·K)
$h$	height, m
$K_d$	discharge coefficient
$M$	mass flow rate, kg/s
$P$	pressure, kPa
$P_b$	back pressure, kPa
$R$	mass flow rate ratio
$T$	temperature, K
$v$	specific volume, m <sup>3</sup>
$\alpha$	homogeneous void fraction
$\eta$	pressure ratio
$\rho$	density, kg/m <sup>3</sup>
$\omega$	compressible flow parameter
ID	inner diameter, m
MAP	maximum allowable pressure, kPa
MAWP	maximum allowable working pressure, kPa
OD	outer diameter, m
RV	relief valve

# CHAPTER 1

## INTRODUCTION

### 1.1 General Introduction

Flexible and stretchable materials have been starting investigated all around the world, as well as the micro-system technologies (MST) have grown at a faster rate. Those devices are presented in micro- and nano- scale so as to be easily integrated into rigid machines, robotic and biomedical applications. For biomedical applications, flexible and stretchable materials will be suggested especially for wearable and implantable devices, since the integrated components were evolved from rigid to flexible and stretchable devices. And nowadays humanoid robots with better sensing capabilities have been discovered to do effective interaction between people and robots.

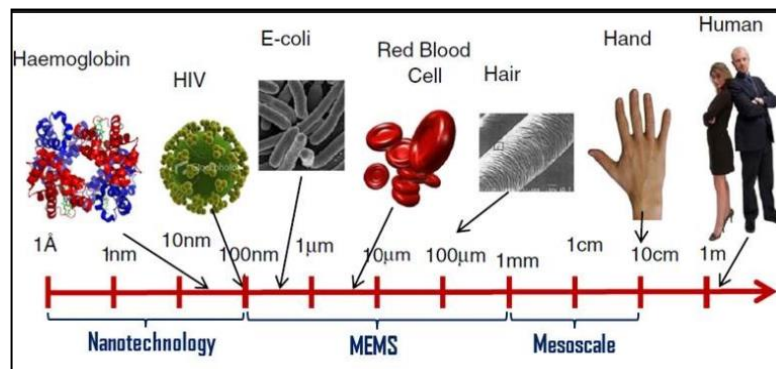


Figure 1.1: Dimension Scale of MEMS and Nanotechnology (Nguyen et al, 2013).

Microelectromechanical system (MEMS) is one of the micro-system technologies that have the functions of sensing and actuation with the computation and communication to locally control physical parameters at micro scale. It can convert mechanical strain to produce electricity or vice versa. In order to produce electricity, energy harvesting method is strongly introduced instead of using battery with lot of shortcomings. Lot of the devices can become wireless products and always being self-powered by themselves. Furthermore, not only energy harvesting method can be used in robotic and biomedical applications, but also in our daily devices such as sustainable energy system. Our current lifestyle has been improved with the advanced technology and demands for more electricity to power those high technologies.

## **1.2 Importance of the Study**

Energy harvesting method is introduced rapidly around the world in order to replacing the usage of batteries which have limited lifetime. Lot of electronic products and devices cannot be functioned without battery, in other word, wireless products are still investigated. Although this method can replace the use of batteries, it is only suitable for those low power applications, and some nature environmental sources are not stable and limited. Once the source is gone, the device cannot be powered and people will still have strong dependence on using batteries so that can make sure the product is functioning. Therefore, the research for innovative energy harvester is needed to put more effort for long term supply without batteries.

## **1.3 Problem Statement**

Technologies in today are kept changing and ongoing to explore more advanced products in the future such as wireless sensors, robotic and automation, biomedical devices and so on. Those technologies have been increased in a faster rate but still not keep pace with that in overseas. In our country, lot of electronic products have strong dependent on the use of battery that cannot be recycled after use. This is one of the problems as battery has many disadvantages like short life time, limited power storage, maintenance issues, large weight and size. Even though it is convenient, battery is no longer a suitable way to provide larger power. Therefore, energy harvesting method will be investigated in this project.

This research is to investigate the raindrop energy harvesting to obtain electricity in order to power the electronic devices. The second problem is the rain conditions including the rain intensities, the size of the rain droplets, the velocity and the height for rain droplets to fall. Those parameters can be assumed as the force placing on the stretchable sensor, in which they can affect the values of energy and power produced by an energy harvester and also affects the operation of a powered device.

The third problem is how suitable a rectifier circuit can be developed to store the extra energy for later use. Although Malaysia has better rainfall, there is necessary to have a battery bank to store the energy in case there have few days

without rain. This problem will be discussed in further improvement part about the method of storing extra energy.

#### **1.4 Aims and Objectives**

The aim of this research is to study the characteristic of raindrop harvesting based on stretchable electronic through the vibration of the flexible sensor to collect the electricity.

In order to study the performance of raindrop energy harvesting, some objectives are required.

1. The concept of electromagnetic energy harvesting is referred to be applied on raindrop harvesting by converting mechanical energy to electrical energy through the simulation.
2. Different placement of Neodymium (NdFeB) magnet on the Ecoflex sensor will be studied, as well as the quantity of magnets being used and the number of turn of spiral coil.
3. The applications of this stretchable electronic using energy harvesting method will be investigated in different areas and the method of storing extra energy will be discussed.

#### **1.5 Scope and Limitation of the Study**

As mentioned in the previous, the soft tactile sensor can be powered by energy harvesting techniques either coming from nature environment or human sources. In this project, a kinetic energy harvesting from human source, in which it is so called magnetic induction energy, will be adopted to power the soft sensor by generating electric energy via mechanical motion or vibration. This is so called electromagnetic energy.

Furthermore, the project will also focus on all enhancements of the prototype, such as the dimension of the sensor and the shape of the coil, the properties of the base material and so on. Different applied forces in different direction will be adopted to figure out the performance of stretchable sensor.

Since there are lot of applications for using tactile sensor, the scope of the research was more focus on the development of biomedical devices. Ambient temperature and humidity were assumed to be constant.

## **1.6 Outline of the Report**

The report is composed of few chapters, which consist of introduction, literature review, research methodology, result and discussion, and conclusion, respectively. The introduction will display the background of tactile sensing using eco-flex soft sensor and some problem statement based on the objectives of the research. Literature review in chapter 2 is about the past researches that are relevant to the topic and some concepts to help in the forthcoming design. The methodology applied in the report will be further described in the chapter 3. Some recommendation and future improvement are discussed to provide some ideas for the purpose of further design.

## CHAPTER 2

### LITERATURE REVIEW

#### 2.1 Introduction

In the literature review, there will discuss about some concepts and characteristics of how a tactile sensor using eco-flex soft sensor is being made. According to this topic, some keywords are important and will be strongly explained in the following parts, such as energy harvesting, spiral coil and stretchable materials. Based on the literature review, it can obtain some basic knowledge and ideas to further improve in designing a better soft sensor.

#### 2.2 Energy Harvesting

In the recent year, people keep discovering a large number of new electronic products. Even though they are low power electronic devices, people cannot live without those electronic devices and thus cause the increase in energy consumption. The environment problem is always taken into consideration while designing a new product. Some devices that consume more energy are powered by battery which only has limited lifetime for a period of use and cause the battery needed to prolong its life.

To further improve this problem, the concept of energy harvesting is introduced as it has lot of energy-saving techniques. Energy harvesting is the process of creating the electricity from environmental energy sources and human, storing them for later use. The reason why energy harvesting is attractive is because it can replace the battery or even wall plug and eliminate the use of wire to produce electricity. It is also considered as “free energy” because the energy can be obtained from the natural environment without paying cost. They are having maintenance-free and is available throughout the lifetime of the application(Hannan et al., 2014).

There are some energy harvesting methods with two main different types as shown in Figure 2.1. Those energy harvesting devices are used to power various sensor and some wireless sensor network systems.

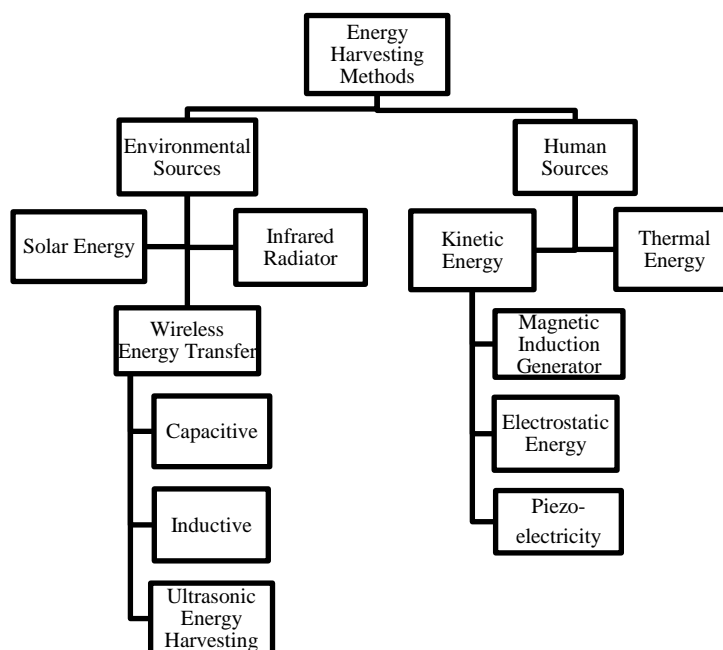


Figure 2.1: Energy Harvesting Methods(Hannan et al., 2014).

### 2.2.1 Environmental Sources

Environmental energy harvesting is a process that gathering the natural energy sources surrounding us and convert them into useable electricity to power the device. It consists of solar energy captured by solar cell, infrared radiator and wireless energy transfer which are capacitive coupling link, inductive energy harvesting and ultrasonic energy harvesting.

#### 2.2.1.1 Solar Energy

In Malaysia, solar energy is always recommended to be used for the purpose of environment protection due to the abundant sunshine throughout the year. Since the average daily solar radiation in Malaysia is about  $4500 \text{ kWh/m}^2$  and the average daily sunshine duration about 12 hours, our country has highly potential for solar power generation (Aziz et al., 2016). It can also be noticed surrounding us that the solar cell is always present either in the house or in the office, like using solar device to power the water heater and the calculator which has PV cell mounted on the top.

Solar energy can be captured from sunlight via photo sensor, diode or solar panel. Photovoltaic system consists of several solar cells made from different types

of semiconductor materials such as crystalline silicon, amorphous silicon and so on. The concept of the solar panel shown in Figure 2.2 is that it will receive photon (sun light) and convert it into electron before powering the devices. It consists of anode and cathode on two side of the solar cell, as well as the front contact, anti-reflecting and black contact. When the solar cell is placed under the sun, it absorbs the sun light which is proportional to the amount of sun radiation, it will release the electron while the electrical field is formed between anode and cathode. The electrons are thus captured and become electric current used as electricity to power the load (Hannan et al., 2014).

However, the sun intensity is only higher during the day instead of night, so it is necessary to have a backup plan like storing the energy sources in the supercapacitor or using the solar cell to charge the batteries.

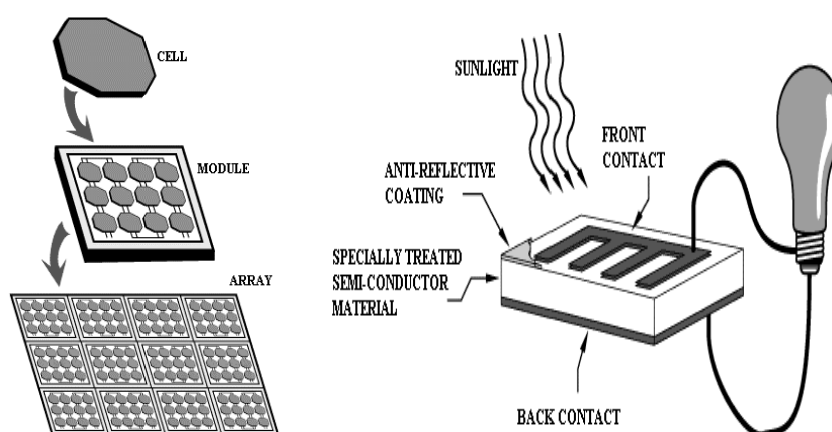


Figure 2.2: The Structure and the Operation of Solar Cell (Knier, 2008).

### 2.2.1.2 Infrared Radiator

Infrared radiation is one of the energy harvesting methods with longer wavelength than the wavelength of visible light which is in the range between  $850\text{ nm}$  and  $1100\text{ nm}$  (Murakawa et al., 1999). It is normally used to power the large implanted biomedical devices such as cardiac, pacemakers, deep brain stimulators for Parkinson's diseases and so on (Hannan et al., 2014).

Figure 2.3 shows that a photovoltaic cell mounted outside the body skin absorbs the infrared light to power the implanted equipment which is attached to the cell. The operation of this wireless energy system is that the photovoltaic cell detects

and absorbs the infrared light, thus converts the infrared radiation into electrical energy which can be used for recharging the battery as well as powering the implanted device. The rechargeable battery can store the electric power in case there is no radiation (Murakawa et al., 1999).

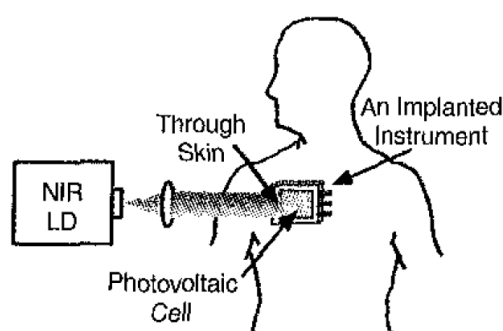


Figure 2.3: Wireless Energy System Powered by Infrared Radiation (Murakawa et al., 1999).

There are few types of photodetectors available in infrared with high sensitivity like silicon PIN photodiode, Si monocrystal solar cell, InGaAs and Ge. Solar cell with the efficiency of 17 % which is lower than Si PIN photodiode with the efficiency of 19 % will be easier to apply in large devices (Murakawa et al., 1999).

### 2.2.1.3 Wireless Energy Transfer

Wireless energy transfer until today is a vigorous energy harvesting method that is used to power implanted biomedical device at a short wireless communication (Hannan et al., 2014). It comprises three main methods which are ultrasonic energy harvesting, capacitive coupling link and inductive energy harvesting.

#### 2.2.1.3.1 Ultrasonic Energy Harvesting

Ultrasonic energy harvesting is the method that is used to harvest electrical energy from an ultrasonic transducer. The energy harvester is designed based on two degree-of-freedom MEMS that features the simulated resonance modes in x-axis and y-axis, generating the electrical energy through the transducer. It also can be designed as a 3

degree-of-freedom MEMS which has three resonance modes in the in-plane and out-plane (z-axis)(Fowler et al., 2013).

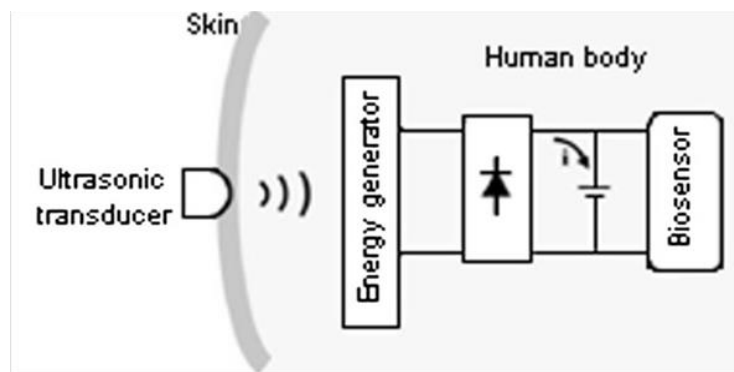


Figure 2.4: Ultrasonic Energy Harvesting Method with Implanted Device (Hannan et al., 2014).

Figure 2.4 is the ultrasonic energy harvesting mechanism which the energy harvester is mounted on the skin with the biosensor. The ultrasonic transducer will emit ultrasonic wave for the MEMS to absorb and convert into electrical energy to power sensor inside the body (Hannan et al., 2014). This method is quite safe to be used for human body which has been applied in few years ago, for instance a device was designed using pulsed ultrasound to create a miniature currents in piezoelectric devices (Phillips et al., 2003). However, there still have several drawbacks needed to be improved such as low energy is harvested and large size due to MEMS devices.

### 2.2.1.3.2 Inductive Energy Harvesting

An inductive coupling link system has two coils as communication tools for implanted biomedical devices in short distance. One of the coils is located outside the body to transmit the power up to milliwatts to another coil attached to implant sensor which can refer to the system shown in Figure 2.5. Primary coil is considered as reader coil whereas secondary coil located inside body is connected to implant sensor (Hannan et al., 2014).

When the alternate current flows through the primary circuit, in which a magnetic field is generated and the power is transferred stably through the body tissues without wire connection, an electromotive force is induced due to the change of magnetic flux at secondary coil. This technology has the advantages of bidirectional data transmission without using radio-frequency (RF) transmitter or

receiver. RF transmitter has highest power consumption compared to other components of implantable sensor. In order to enable saving a large amount of energy, the data transmission without the use of RF transmitter is introduced and this kind of techniques is called backscattering (Olivo et al., 2011).

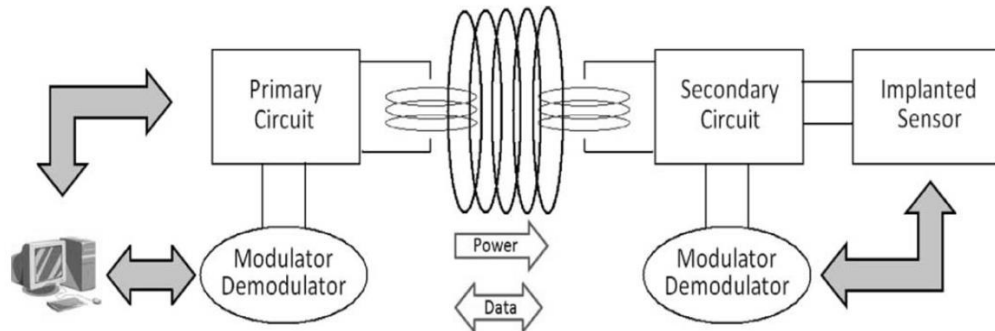


Figure 2.5: An Inductive Coupling Link System with Bidirectional Data Transmission (Olivo et al., 2011).

Due to the advantage of bidirectional data transmission between reader coil and implanted sensor, inductive coupling link is suitable for low invasive implanted biomedical devices. This system usually uses a lower frequency at the range of few megahertz and below in order to avoid body tissue heating by reducing the power absorption and thus inducing a high transmission efficiency (Hannan et al., 2014). A biomedical device was produced by applying the concept of inductive coupling link system. It is neurostimulator “RestoreUltra” for stimulating the spinal cord with a rechargeable battery (Olivo et al., 2011).

### 2.2.1.3.3 Capacitive Coupling Link

Capacitive coupling link system comprises two parallel plates acting as capacitors which are transmitting plate located outside the body skin and receiving plate connected to implanted devices. Similar to inductive coupling link system having magnetic field to transmit data, capacitive energy harvesting applies electric field to transfer power as well as the data through the body tissues that behaves as a dielectric medium (Sawma et al., 2015).

The advantage of capacitive coupling link system is that it has high positioning flexibility, an electrode unit with high design flexibility and an electrode unit that do not generate heat. Although it is efficient in achieving higher power and allow the electrode to be located near the battery, the plates may also increase the temperature of body tissue causing the patient uncomfortable (Hannan et al., 2014).

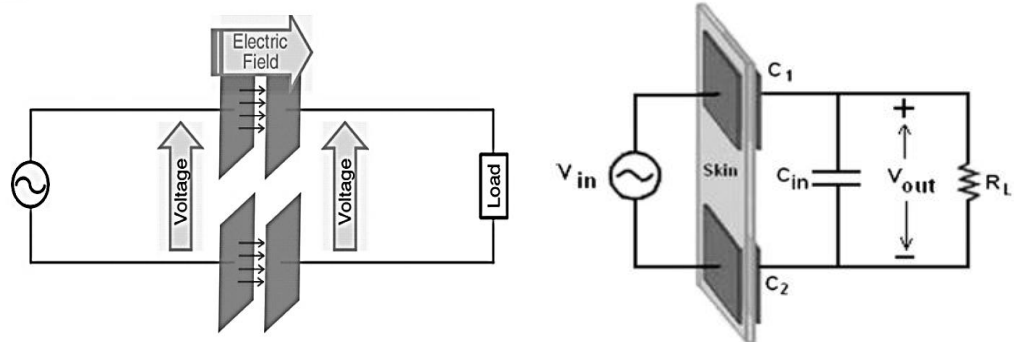


Figure 2.6: The Simplified Capacitive Coupling Link (Hannan et al., 2014).

## 2.2.2 Human Sources

Thermal energy and kinetic energy are considered as human energy harvesting as they produce electricity from human temperature, motion, vibration and so on. The different levels of power are based on the activities done by human. For instance, sleeping can produce  $81\text{ mW}$  of the power, whereas human motion can produce approximately  $1630\text{ mW}$  of the power. There have three different types of kinetic energy which are magnetic induction generator, electrostatic energy and piezoelectricity.

### 2.2.2.1 Thermal Energy

Thermal energy harvester is a technique to create the power based on the different temperature in the environment. This process is so called Seebeck effect where the temperature difference between two dissimilar thermoelectric will produce a small voltage difference up to microvolts. The voltage difference can be larger by increasing the temperature difference.

Figure 2.7 shows that there is a thermoelectric module with two different temperatures consists of large amount of thermocouple and thermopile connected in

parallel form. Normally the thermoelectric module will be connected between power transistor and heat sink to recycle some energy otherwise it will lose as heat. Some of them will convert the heat to produce minimal power which is sufficient to some implanted biomedical devices or store the energy in the durable storage components like supercapacitor. Figure 2.8 has shown the Seebeck effect of the thermoelectric module.

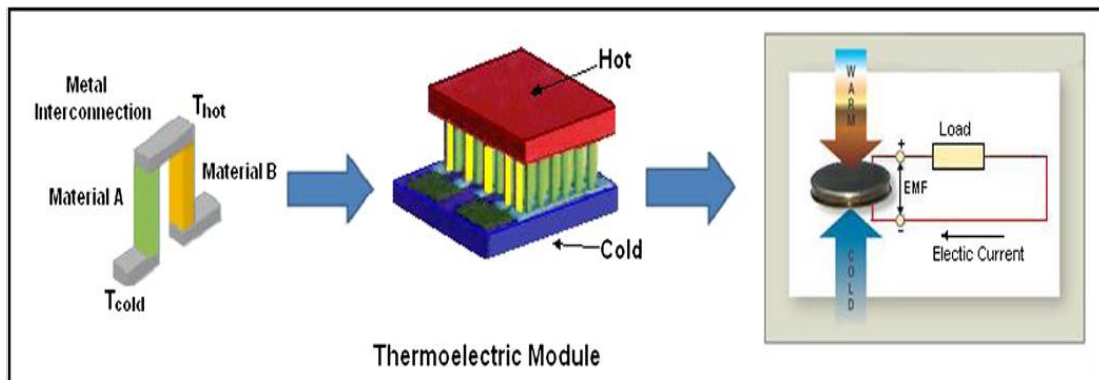


Figure 2.7: The Equivalent Scheme of Thermoelectric Module with Thermopile (Hannan et al., 2014).

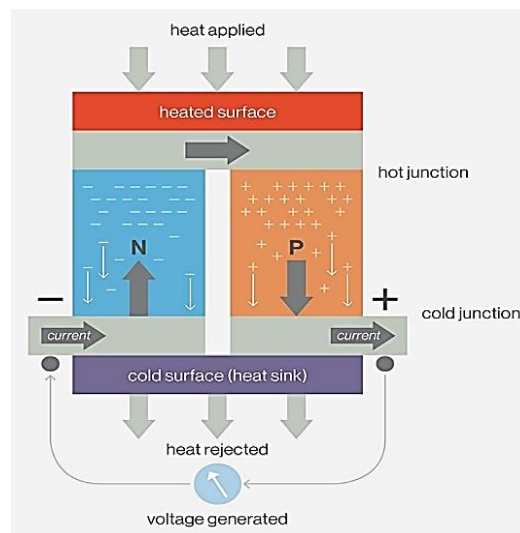


Figure 2.8: Seebeck Effect of the Thermoelectric Module.

### 2.2.2.2 Kinetic Energy

As mentioned in the previous, activities done by human will produce specific power no matter they are running, walking or even sleeping. By providing the kinetic energy, there have few kinds of energy harvesters to generate the power from human body motion and vibration, such as magnetic induction generator, electrostatic energy and piezoelectricity, which will be discussed in the following.

### 2.2.2.2.1 Magnetic Induction Generator

This energy harvesting method converts the vibratory movement into electromagnetic energy to generate the power for implanted devices. It consists of two types magnetic induction generators with relative motion and rigid body motion, respectively (Hannan et al., 2014). Figure 2.9(a) shows that a relative motion is used while the generating system is fixed whereas Figure 2.9(b) shows a rigid body motion is used on the generator with the vibration by inertia force. Electromagnetic transducers are always used to create electromotive force by the change of magnetic flux.

This technique has been introduced to power quartz wristwatch using Seiko kinetic approach. Citation from Figure 2.10, it uses the concept of the change of magnetic flux over a certain area to generate an electromotive force for the purpose of powering the quartz wristwatch. Through the wrist motion, it will bring the oscillating weight to rotor and induce the electromotive force through the coil. The wristwatch itself enables charging by wrist motion and stores the charge in a common battery (Olivo et al., 2011). Seiko kinetic approach was then applied successfully in many studies like biomedical field. For example, it can be used to charge the pacemaker battery by heartbeat utilization.

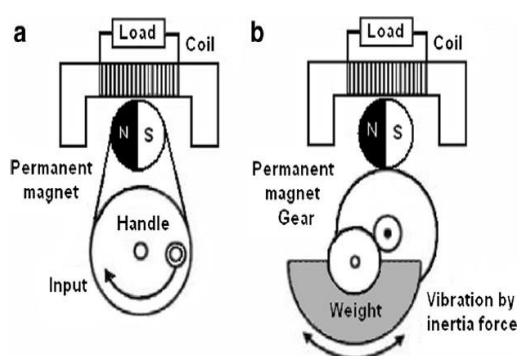


Figure 2.9: Magnetic Induction Generator with Relative Motion and Rigid Body Motion (Hannan et al., 2014).

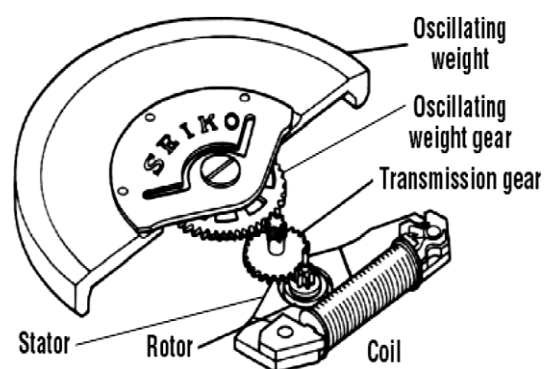


Figure 2.10: Seiko Wristwatch Using Seiko Kinetic Approach (Mitcheson et al., 2008)

Furthermore, the disadvantage of using this electromagnetic energy harvesting is that there is needed to periodically lubricate the moving part between the oscillating weight gear and the magnetic rotor otherwise it will affect the implanted devices to be replaced in the end (Olivo et al., 2011).

### 2.2.2.2.2 Electrostatic Energy

Electrostatic generator converts mechanical vibration to produce electricity and this method is only suitable for low-power implanted biomedical devices whereas it will reduce the efficiency if a high power is required. A variable capacitor based on the electrostatic transducers is used to create electric field and the two plates can be positioned by the mechanical work against external force under two different modes of operation, constant charge and constant voltage, respectively (Hannan et al., 2014).

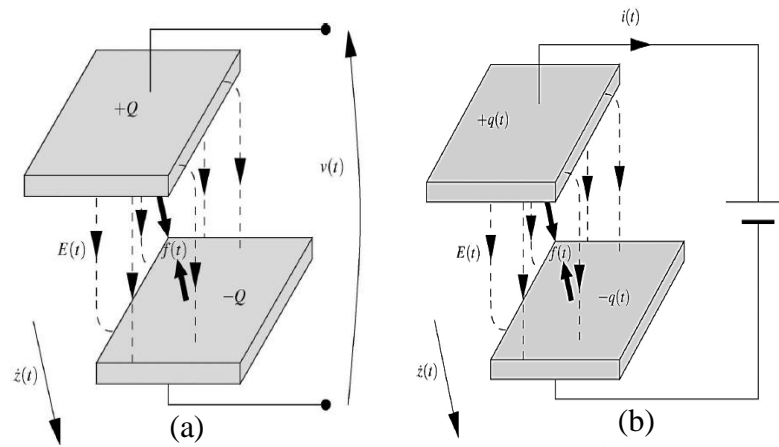


Figure 2.11: The Electrostatic Transducer under the Operation of (a) Constant Charge and (b) Constant Voltage (Mitcheson et al., 2008).

According to the energy density equation due to electric field,

$$u(\text{energy density}) = \frac{1}{2} \frac{CV^2}{Ad} \quad (2.1)$$

where  $A$  is the area of capacitor plates and  $d$  is their separation distance. By replacing the charge  $C = \epsilon_0 \frac{A}{d}$  and voltage  $V = Ed$  across the capacitor, the relationship of electric field and energy density can be figured as below,

$$u = \frac{1}{2} \epsilon_0 E^2 \quad (2.2)$$

When the electrostatic transducer operates under constant charge, the external force varies with the voltage across two parallel plates. The electric field is proportional to the charge and the energy density does not depend on the plate separation while the parallel plates are under normal motion with variable separation. Following by the increase in electrode separation, the potential energy is increased and stored in the large amount of electric field. By moving the plate laterally, the electric field strength is increased as well as the energy density of electric field (Mitcheson et al., 2008).

When the electrostatic transducer operates under constant voltage, the plate separation is increased and thus generates current flowing through the capacitor. If the plates move laterally with fixed separation, the electric field strength will remain constant and the current continues flowing into the circuit (Mitcheson et al., 2008).

### 2.2.2.2.3 Piezoelectricity

Piezoelectricity is the energy harvesting technique using piezoelectric materials to generate an electric energy when there is a mechanical motion, vibration and pressure. The working principle of piezoelectric effect is related to its crystalline material from nature as well as their various properties that might affect the efficiency of piezoelectricity. There also have some artificial crystals formed by chemical compounds such as Barium Titanate, Lead Titanate and Lead Zirconate Titanate (PZT) (Res et al., 2016).

In order to determine whether the piezoelectricity is the best, some parameters are needed to distinguish which can be referred to Table 2.1. By the way, Lead Zirconate Titanate (PZT) is commonly used in designing piezoelectricity due to its properties, for example, easily fabricated to any complex shape, high material strength, long-life service and so on (Res et al., 2016).

Table 2.1: The parameters of piezoelectricity(Res et al., 2016).

Geometry	The most efficient form to produce more energy is tapered shape.
Thickness	More energy is produces with thinner material.
Loading Mode	More energy is produced with increase in mass or force.
Fixation	Fixation at one end will result in more deflection, thus more energy when subjected to external force, than when fixed at two ends.
Structure	Bimorph structures produce double the energy output than unimorph structure.

There was a study done by Ramsay and Clark using a square PZT-5A to provide energy with a larger amount of power that fluctuated from blood pressure.

PZT is a type of piezoceramic and its design depends on the mobility of domains and the polarization and depolarization behaviour (Hannan et al., 2014). Some researchers used piezoceramic within knee replacement implant and orthopaedic implant to generate power. Table 2.2 shows the advantages and disadvantages of using piezoelectricity to generate power for implanted biomedical devices.

Table 2.2: Pros and cons of piezoelectricity(HR, 2015).

Advantages	Disadvantages
<ol style="list-style-type: none"> <li>1. Very high frequency response</li> <li>2. Self-generating without external source</li> <li>3. Ease of use due to small dimensions and large measuring range</li> </ol>	<ol style="list-style-type: none"> <li>1. Not suitable for measurement in static condition</li> <li>2. Need high impedance cable for electrical interface as the device operates with small electric charge</li> <li>3. The output may vary with the temperature variation of piezoelectric material</li> </ol>

### 2.3 Conductive Liquids

A flexible tactile sensor is designed using conductive liquid encapsulated in the microchannel. Considering the stretchiness of the sensor, liquid is a suitable tool to be used as it will not be destroyed during deformation. Compared to copper wire, it will be easily broken while stretching the soft sensor, in which it is not a suitable tool of using conventional rigid metal.

Furthermore, there are some common conductive liquids used to fill the microchannel which are eutectic gallium indium (eGaIn), carbon black, silver, ionic liquid, Galinstan and so on. Eutectic gallium indium (eGaIn) and Galinstan are always used in the soft sensor to fill the microchannel due to their properties such as conductivity and resistivity. (Yildiz et al., 2016)

Eutectic gallium indium is a metal alloy that consists of 75 % of gallium and 25 % of indium. It has higher conductivity due to its low resistivity and hence these properties will cause the sensor more sensitive to the electrical noise and variation in the interface resistance. It will produce electric current flowing throughout the microchannel which consist of conductive liquid and thus transmit the sensor signal to give an output. (Chossat et al., 2013)

Apart from that, another microfluidic used in microchannel is Galinstan which is eutectic liquid metal alloy comprising 68.5 % of gallium, 21.5 % of indium and 10 % of tin. It has excellent electrical conductivity, low melting point and low vapor pressure. (Jin et al., 2015) There is a comparison of the properties of mercury and Galinstan shown in Table 2.3 to prove that Galinstan has lower toxicity than mercury so that it is much safer to be replaced with mercury in some microelectromechanical system (MEMS). The problem using Galinstan is that its surface will have a rapid oxidation in the air causing slow adoption in microscale devices. In order to prevent Galinstan from oxidation, it is needed to keep under an inert environment containing nitrogen or cover by aqueous solution. (Liu et al., 2012)

Table 2.3: The Comparison of Properties of Galinstan and Mercury (Liu et al., 2012).

<b>Property</b>	<b>Galinstan</b>	<b>Mercury</b>
Color	Silver	Silver
Odor	Odorless	Odorless
Boiling point	> 1300 °C	356.62 °C
Melting point	-19 °C	-38.83 °C
Vapour pressure	< $10^{-6} Pa$ at 500 °C	0.1713 Pa at 20 °C
Density	6440 kg/m <sup>3</sup>	13533.6 kg/m <sup>3</sup>
Solubility	Insoluble	Insoluble
Viscosity	$2.4 \times 10^{-3} Pa \cdot s$ at 20 °C	$1.526 \times 10^{-3} Pa \cdot s$ at 25 °C
Thermal conductivity	$16.5 W \cdot m^{-1} \cdot K^{-1}$	$8.541 W \cdot m^{-1} \cdot K^{-1}$
Electrical conductivity	$2.30 \times 10^6 S/m$	$1.04 \times 10^6 S/m$

Last, the reason why conductive liquids are used in stretchable devices instead of using copper wire is that it is deformable metal liquid for large deformation even though copper wire has higher conductivity of  $5.96 \times 10^7 S/m$ . To make Galinstan behaves like other liquid metals, the amount of oxygen is required to reduce below 1 ppm (parts per million, 0.0001 %). However, maintaining Galinstan not to be oxidized is still a challenging problem needed to be solved.

## 2.4 Stretchable Material

The development of functional micro-electromechanical system (MEMS) technology is still challenging and being improved by lot of researches in the area of biomedical system, soft robotic system or even wearable devices. The materials that used to conduct those applications must have highly flexible and stretchable properties that can undergo larger deformation such as polydimethylsiloxane (PDMS) and eco-flex (0030) are the suitable polymers to be used. For instance, an implanted biomedical device which is rigid is hard to attach to the human body skin since the skin is soft and deformable and some of the parts have joints, so that a flexible and stretchable material is needed.

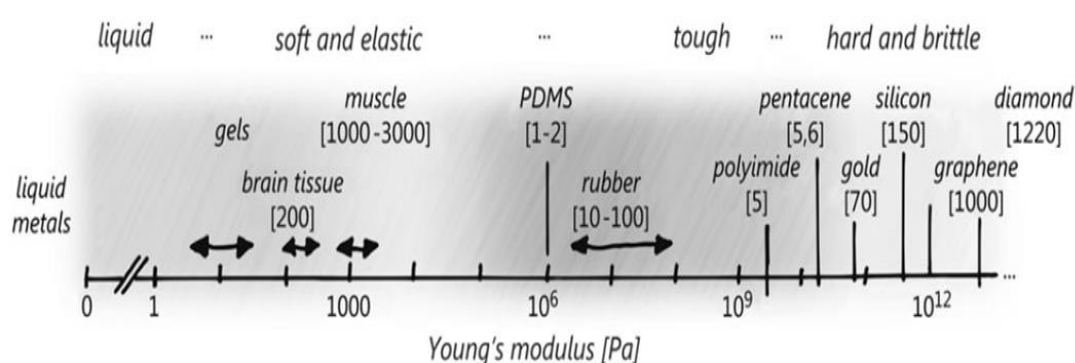


Figure 2.12: Stretchable Electronic Surfaces with Different Values in Young Modulus (Wagner and Bauer, 2012).

Stretchable electronic surfaces consist of viscoelastic, plastic and hard and brittle with different values in Young modulus as shown in Figure 2.12. The Young modulus for Ecoflex (0030) and PDMS are about 69 kPa and 615 kPa respectively, in which can be noticed that Ecoflex is softer than PDMS to be used as a stretchable material (Jin et al., 2015). The materials with higher Young's modulus are difficult to be deformed whereas highly elastic materials are easily stretched in uniaxial, biaxial or radial ways.

To determine the characteristics of PDMS and Ecoflex (0030) of such stretchable materials, their electrical properties can be varied with the applied strain due to the deformation. The change in resistance is varied with the applied strain in different pattern of stretching. Yildiz et al calculate the ratio of displacement which is the ration of the length when the material is being stretched to the initial length when the material is rest. The result showed that the resistance will be increased

comparing to the initial resistance while increasing the stretch strain, in which depends on the magnitude of applied force (Yildiz et al., 2016).

Besides that, different kind of force direction will come out different response. There have few types of strains that might change the electrical properties like normal surface pressure, multi-axial strain, shear force and bending curvature to stretch the soft sensor. And some mechanical parameters will affect the sensor performance such as the width of the microchannel, the thickness of the prototype, the number of turn of the microchannel and so on. Those mechanical will be discussed on the following subtopic about different kind of design of the microchannel(Vogt et al., 2013).

According to the resistance change with respect to the applied strain, the response has shown that Ecoflex (0030) has higher linearity with low hysteresis. Ecoflex has the advantage of being stretched up to 100 % whereas PDMS will not function.

## 2.5 Spiral Coil

The performance of a soft sensor not only depends on what conductive liquid is being filled in the microchannel, but also the geometry of microchannel like channel dimensions and cross-sectional area of microchannel has to take into consideration. There have some various design of coil shapes shown in Figure 2.13, such as circular coil, square coil, serpentine coil and so on.

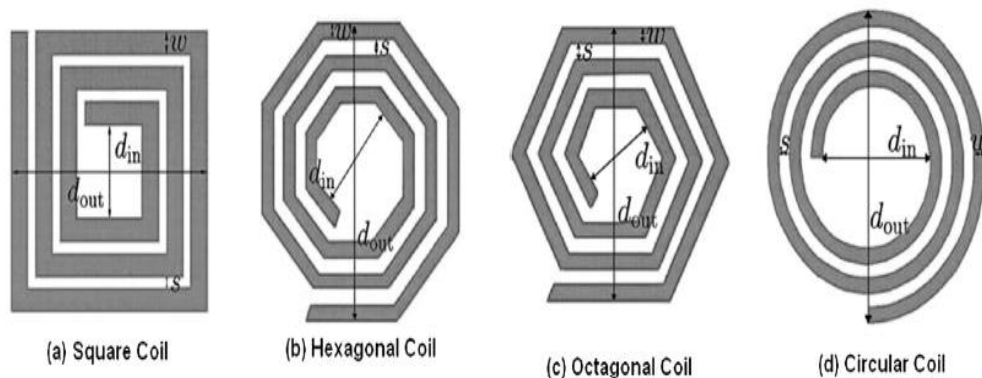


Figure 2.13: Different Pattern of Coil Shape for Microchannel (Hannan et al., 2014).

When the sensor is stretched under certain strain, the electrical resistance of microchannel is increased because the channel length is increased whereas its cross-

sectional area is reduced (Park et al., 2012). This relationship can be defined by the following equation.

$$R = \rho \frac{L}{A} \quad (2.3)$$

Where  $R$  is the resistance of microchannel,  $\rho$  is the electrical resistivity of conductive liquid,  $L$  and  $A$  are the length and cross-sectional area of microchannel, respectively. The change in resistance ( $\Delta R$ ) against the strain ( $\epsilon$ ) can be figured out as follow:

$$\Delta R = R - R_0 = \rho \frac{L+\Delta L}{(\omega+\Delta\omega)(h+\Delta h)} - \rho \frac{L}{\omega h} \quad (2.4)$$

The Poisson's ratio of the elastomeric material is the ratio of transverse strain to axial strain given by the formula,  $\nu = \left| \frac{\epsilon_2}{\epsilon_1} \right|$ , where  $\epsilon_1 = \frac{\Delta L}{L}$  and  $\epsilon_2 = \frac{\Delta\omega}{\omega}$ . So,  $\Delta\omega$  and  $\Delta L$  can be replaced to  $-\nu\epsilon\omega$  and  $-\nu\epsilon L$ . Hence, the equation (2) can be simplified to

$$\Delta R = \frac{\rho L}{\omega h} \left[ \frac{(1+2\nu)\epsilon - \nu^2\epsilon^2}{(1-\nu\epsilon)^2} \right] \quad (2.5)$$

## 2.6 Summary

In this chapter, different energy harvesting methods are given a brief explanation. Although it is only suitable for low power device, it can replace battery to self power and acts as a wireless product. Stretchable material filled with conductive liquid is also introduced as well instead of using rigid component that is difficult to attach in many research areas, especially biomedical area because they are flexible and deformable like an electronic skin. Lastly, the shape and dimension of the coil that is used to fill with the conductive liquid is taken into account as it can affect how much the electricity that the device can produce.

## CHAPTER 3

### METHODOLOGY AND WORK PLAN

#### 3.1 Introduction

In this section, it will show how to model the magnetic field surrounding a stretchable eco-flex material with EGaIn liquid inside the spiral coil and some Neodymium magnets using Comsol Multiphysics 5.3a software to do the simulation. A brief concept about the experiment will be discussed, as well as the modelling instructions about Comsol setting.

#### 3.2 Brief Concept about Raindrop Energy Harvesting on Stretchable Electronic.

This raindrop energy harvesting applies the concept of electromagnetic energy harvesting on a stretchable prototype to convert the motion or vibration into electricity. The experiment setup will use some Neodymium magnets which have stronger magnetic and attaches with the prototype so that it will generate some electromagnetic energy by cutting the magnetic flux when there is a vibratory movement.

From Figure 3.1, a box with many holes at the bottom is used to produce water droplets and different sizes of holes are made to produce different size of water droplets to fall on the top of the prototype. Syringe can be used to create water droplets also but it might not get the constant output. The motion of falling raindrop can be act as a force or pressure on prototype to create vibration and generate electricity.

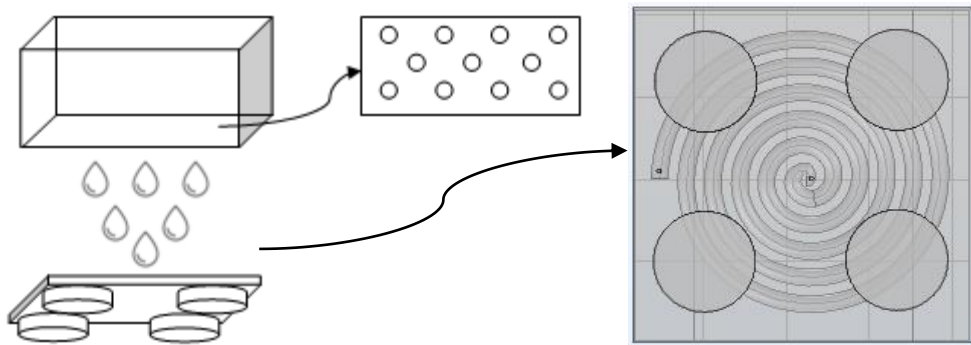
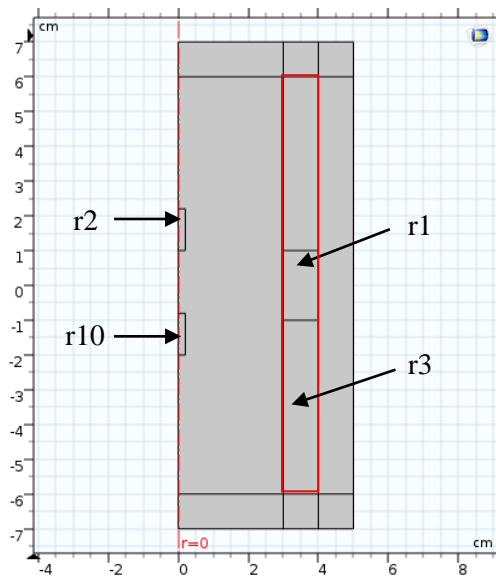


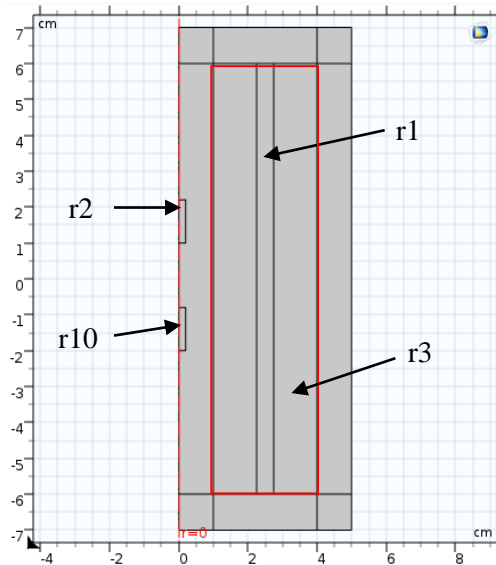
Figure 3.1: Experimental Setup.

In Comsol software, the 2D axial symmetric models are drawn as shown in Figure 3.2 and Figure 3.3, in which there are two different methods to perform. To study the performance of the model, the spiral coil filled with EGaIn liquid is moving in vertical and horizontal direction to cut the magnetic flux generated by the Neodymium magnets. The result can be observed in Chapter 4 with different characteristics.



r1	Spiral coil filled with EGaIn liquid
r2,r10	Neodymium magnets
r3	Eco-flex 0030
r4-r9	Air

Figure 3.2: Stretchable Prototype in 2D Axial Symmetric Model where the Coil is moving in Vertical Direction.



r1	Spiral coil filled with EGaIn liquid
r2,r10	Neodymium magnets
r3	Eco-flex 0030
r4-r9	Air

Figure 3.3: Stretchable Prototype in 2D Axial Symmetric Model where the Coil is moving in Horizontal Direction.

### 3.3 Flowcharts for Modelling Instructions of the Simulations

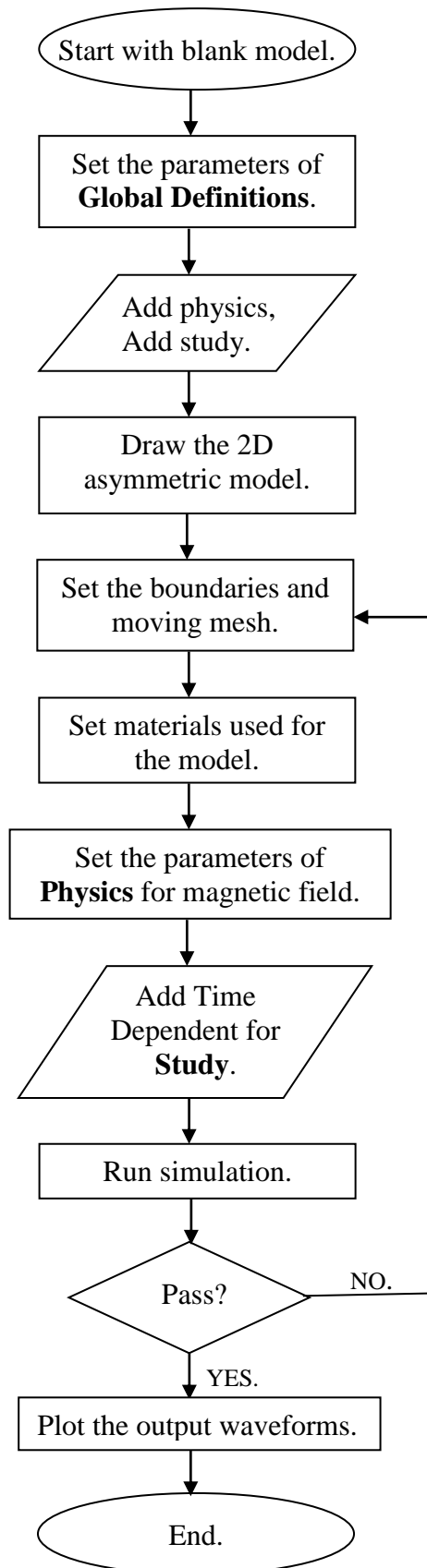


Figure 3.4: The flowchart for both simulations.

Figure 3.4 shows the flowchart for both simulations which are the modelling instruction illustrated in section 3.4 and 3.5. All the parameter settings are the same whereas the parameters for geometry and the value for moving mesh, as well as the boundaries setting, are different. It is because one of the simulations is that spiral coil is moved in vertical direction and another one is the coil moved in horizontal coil.

### 3.4 Modelling Instruction for Moving Coil in Vertical Direction with Two Fixed Neodymium Magnets

From the **File** menu in Comsol Multiphysics 5.3a, choose **New**.

- **NEW**  
In the **New** window, click **Blank Model**.
- **BLANK MODEL**
  1. On the **Home** toolbar, click **Component** and select **2D Axisymmetric**.
  2. In the **Add Physics**, select **AC/DC>Magnetic Fields (mf)** and click **Add to Component**.
  3. In the **Add Study**, select **Preset Studies>Stationary** and click **Add Study**.
- **GLOBAL DEFINITIONS**
  1. In Parameters part, set the following data in the parameters table.

Table 3.1: The Parameters of Global Definitions.

Name	Expression	Value	Description
f0	4[Hz]	4 Hz	Frequency of an oscillating coil
T0	1/f0	0.25 s	Time period of an oscillating coil
t	0[s]	0 s	-

- **GEOMETRY**
  1. On the **Geometry** toolbar, click **Rectangular**.
  2. In the **Setting** window for rectangular, locate the **Size and Shape** section and the **Position** section.
  3. To create the model as shown in Figure 3.2, all the widths and heights are presented in the Table 3.2.
  4. After plotting the rectangular based on the width and height, click **Build Selected** in the **Setting** window.

Table 3.2: The Parameters of Geometry for Figure 3.2.

Geometry	Size and Shape (cm)		Position (cm)	
Rectangular 1 (r1)	Width	1.0	r	3
	Height	2.0	z	-1
Rectangular 2 (r2)	Width	0.2	r	0
	Height	1.2	z	1
Rectangular 3 (r3)	Width	1.0	r	3
	Height	12.0	z	-6
Rectangular 4 (r4)	Width	3.0	r	0
	Height	12.0	z	-6
Rectangular 5 (r5)	Width	2.0	r	3
	Height	1.0	z	6
Rectangular 6 (r6)	Width	2.0	r	3
	Height	1.0	z	-7
Rectangular 7 (r7)	Width	1.0	r	4
	Height	14.0	z	-7
Rectangular 8 (r8)	Width	3.0	r	0
	Height	1.0	z	6
Rectangular 9 (r9)	Width	3.0	r	0
	Height	1.0	z	-7
Rectangular 10 (r10)	Width	0.2	r	0
	Height	1.2	z	-2

5. On the **Geometry** toolbar, click **Booleans and Partitions** and choose **Union**.
  - Select rectangular 1 (r1) and rectangular 3 (r3), and label it as Union 1.
  - Select rectangular r2 and r4-r10, and label it as Union 2.
  - Click **Build Selected** after done selecting.

- DEFINITIONS

1. In **Definitions** toolbar, click **Explicit** and label as *Coil Boundaries* in **Settings** window.
  - Select four boundaries of rectangular 1 (r1) which are boundary 37, 38, 40 and 43.
2. Click **Explicit** again, label as *Continuity Boundaries*.
  - Select boundary 42, 43 and 44.
3. In the same toolbar, click **Pairs** and select **Identity Boundary Pair**.
  - Select boundary 20, 21, 23 and 27 as Source Boundaries.
  - Select boundary 35, 36, 37, 39, 41, 42, 43 and 44 as Destination Boundaries.
4. Choose **ALE** in **Definitions** toolbar, click **Moving Mesh** and select **Prescribed Deformation** for three times.  $dx$  in R direction is set as 0.

Table 3.3: The Parameters for Prescribed Deformation.

Prescribed Deformation	Domain Selection	$dx$ in $Z$ direction (meter in unit)
1	12	$30[\text{mm}] * \sin(2 * \pi * f_0 * t)$
2	13	$30[\text{mm}] * \sin(2 * \pi * f_0 * t) * (6[\text{cm}] - Z) / 5[\text{cm}]$
3	11	$30[\text{mm}] * \sin(2 * \pi * f_0 * t) * (6[\text{cm}] + Z) / 5[\text{cm}]$

5. Choose **Infinite Element Domain**  .
  - Select Domain 1 and Domain 5-10.

- **MATERIALS**

1. On the **Home** toolbar, click **Add Material** for the model.
2. Choose the materials for certain domains which can refer to Table 3.4.

Table 3.4: The Material of Geometry for each Domain.

Domain selection	Material
1-2, 5-10	Air
3 and 4	Neodymium [solid]
12	Water, liquid
11 and 13	PDMS, Polydimethylsiloxane

3. For domain 12, rename the material and type **EGaIn liquid** in the Label text field in **Settings** window.
4. For domain 11 and 13 which are set as PDMS, change the Young Modulus to **69 kPa** in the **Settings** window.

- **MAGNETIC FIELDS (MF)**

1. On the **Physics** toolbar, click **Domains** and choose **Ampere's Law**.
2. Select Domain 3 and 4.
3. In the **Settings** window for Ampere's Law, locate the **Magnetic Field** section.
4. From the **Constitutive relation** list, choose **Remanent flux density** and specify the  $B_r$  vector as

0	R
0	PHI
1.2 [T]	Z

5. Click **Domains**, choose **Coil** and select Domain 12
6. In the **Settings** window for Coil, locate the **Coil** section
7. From the **conductor model** list, choose **Homogenized multi-turn** and specify the coil current as  $I_{coil} = 0 \text{ A}$ .

8. From the **Homogenized Multi-Turn Conductor** section, type **5.5** in the **Number of turn** text field.
  9. On the **Physics** toolbar, choose **Pairs** and select **Continuity**.
- **STUDY**
    1. On the **Study** toolbar, click **Study Step** and choose **Time Dependent**.
    2. In the **Settings** window for time dependent, locate **Study Settings** section.
    3. Specify the times as *range(0,T0/100,T0)* in the text field.
    4. Go back to the **Settings** window for study and click **Compute** to run the simulation.
  - **RESULTS**
    1. **3D Plot Group**
      - In the **Results** toolbar, click **3D Plot Group**, choose **Surface** and label it as **Magnetic Flux Density Norm**.
      - Choose **Contour** as well and thus click **Plot** in Settings window.
    2. **1D Plot Group**
      - In the **Results** toolbar, click **1D Plot Group**, choose **Global** and label it as **Coil Induced Voltage**.
      - Locate the **Plot Settings** section, and label the x-axis as *Time (s)* and y-axis as *Coil voltage (V)*.
      - Thus click **Plot** to get the output waveform.
    3. **Animation**
      - In the **Results** toolbar, click **Animation** and choose **Player**.
      - In the **Settings** window, click **Show Frame**.

### 3.5 Modelling Instruction for Moving Coil in Horizontal Direction with Two Fixed Neodymium Magnets

From the **File** menu in Comsol Multiphysics 5.3a, choose **New**.

- NEW

In the **New** window, click **Blank Model**.

- BLANK MODEL

1. On the **Home** toolbar, click **Component** and select **2D Axisymmetric**.
2. In the **Add Physics**, select **AC/DC>Magnetic Fields (mf)** and click **Add to Component**.
3. In the **Add Study**, select **Preset Studies>Stationary** and click **Add Study**.

- GLOBAL DEFINITIONS

1. In Parameters part, set the following data in the parameters table.

Table 3.5: The Parameters of Global Definitions.

Name	Expression	Value	Description
f0	4[Hz]	4 Hz	Frequency of an oscillating coil
T0	1/f0	0.25 s	Time period of an oscillating coil
t	0[s]	0 s	

- GEOMETRY

1. On the **Geometry** toolbar, click **Rectangular**.
2. In the **Setting** window for rectangular, locate the **Size and Shape** section and the **Position** section.
3. To create the model as shown in Figure 3.3, all the widths and heights are presented in the Table 3.6.
4. After plotting the rectangular based on the width and height, click **Build Selected** in the **Setting** window.

Table 3.6: The Parameters of Geometry for Figure 3.3.

Geometry	Size and Shape (cm)		Position (cm)	
Rectangular 1 (r1)	Width	0.5	r	2.25
	Height	12.0	z	-6
Rectangular 2 (r2)	Width	0.2	r	0
	Height	1.2	z	1
Rectangular 3 (r3)	Width	3.0	r	1
	Height	12.0	z	-6
Rectangular 4 (r4)	Width	1.0	r	0
	Height	12.0	z	-6
Rectangular 5 (r5)	Width	4.0	r	1
	Height	1.0	z	6

Rectangular 6 (r6)	Width	4.0	r	1
	Height	1.0	z	-7
Rectangular 7 (r7)	Width	1.0	r	4
	Height	14.0	z	-7
Rectangular 8 (r8)	Width	1.0	r	0
	Height	1.0	z	6
Rectangular 9 (r9)	Width	1.0	r	0
	Height	1.0	z	-7
Rectangular 10 (r10)	Width	0.2	r	0
	Height	1.2	z	-2

5. On the **Geometry** toolbar, click **Booleans and Partitions** and choose **Union**.
  - Select rectangular 1 (r1) and rectangular 3 (r3), and label it as Union 1.
  - Select rectangular r2 and r4-r10, and label it as Union 2.
  - Click **Build Selected** after done selecting.

- DEFINITIONS

1. In **Definitions** toolbar, click **Explicit** and label as *Coil Boundaries* in **Settings** window.
  - Select four boundaries of rectangular 1 (r1) which are boundary 38, 39, 40 and 41.
2. Click **Explicit** again, label as *Continuity Boundaries*.
  - Select boundary 37, 40 and 43.
3. In the same toolbar, click **Pairs** and select **Identity Boundary Pair**.
  - Select boundary 20, 21, 23 and 27 as Source Boundaries.
  - Select boundary 35, 36, 37, 39, 40, 42, 43 and 44 as Destination Boundaries.
4. Choose **ALE** in **Definitions** toolbar, click **Moving Mesh** and select **Prescribed Deformation**.  $dx$  in Z direction is set as 0.

Table 3.7: The Parameters for Prescribed Deformation.

Prescribed Deformation	Domain Selection	$dx$ in R direction (meter in unit)
1	12	$0.1[\text{mm}] \cdot \sin(2 \cdot \pi \cdot f_0 \cdot t)$
2	13	$0.1[\text{mm}] \cdot \sin(2 \cdot \pi \cdot f_0 \cdot t) \cdot (4[\text{cm}] - Z) / 1.25[\text{cm}]$
3	11	$0.1[\text{mm}] \cdot \sin(2 \cdot \pi \cdot f_0 \cdot t) \cdot (1[\text{cm}] + Z) / 1.25[\text{cm}]$

5. Choose **Infinite Element Domain**  .
  - Select Domain 1 and Domain 5-10.

- MATERIALS

1. On the **Home** toolbar, click **Add Material** for the model.

2. Choose the materials for certain domains which can refer to Table 3.8.

Table 3.8: The Material of Geometry for each Domain.

Domain selection	Material
1-2, 5-10	Air
3 and 4	Neodymium [solid]
12	Water, liquid
11 and 13	PDMS, Polydimethylsiloxane

3. For domain 12, rename the material and type *EGaIn liquid* in the Label text field in **Settings** window.
  4. For domain 11 and 13 which are set as PDMS, change the Young Modulus to **69 kPa** in the **Settings** window.
- MAGNETIC FIELDS (MF)
    1. On the **Physics** toolbar, click **Domains** and choose **Ampere's Law**.
    2. Select Domain 3 and 4.
    3. In the **Settings** window for Ampere's Law, locate the **Magnetic Field** section.
    4. From the **Constitutive relation** list, choose **Remanent flux density** and specify the  $B_r$  vector as
 

0	R
0	PHI
1.2 [T]	Z
    5. Click **Domains**, choose **Coil** and select Domain 12
    6. In the **Settings** window for Coil, locate the **Coil** section
    7. From the **conductor model** list, choose **Homogenized multi-turn** and specify the coil current as  $I_{coil} = 0 A$ .
    8. From the **Homogenized Multi-Turn Conductor** section, type **5.5** in the **Number of turn** text field.
    9. On the **Physics** toolbar, choose **Pairs** and select **Continuity**.
  - STUDY
    1. On the **Study** toolbar, click **Study Step** and choose **Time Dependent**.
    2. In the **Settings** window for time dependent, locate **Study Settings** section.
    3. Specify the times as *range(0,T0/100,T0)* in the text field.
    4. Go back to the **Settings** window for study and click **Compute** to run the simulation.

- RESULTS
  1. 3D Plot Group
    - In the **Results** toolbar, click **3D Plot Group**, choose **Surface** and label it as **Magnetic Flux Density Norm**.
    - Choose **Contour** as well and thus click **Plot** in Settings window.
  2. 1D Plot Group
    - In the **Results** toolbar, click **1D Plot Group**, choose **Global** and label it as **Coil Induced Voltage**.
    - Locate the **Plot Settings** section, and label the x-axis as **Time (s)** and y-axis as **Coil voltage (V)**.
    - Thus click **Plot** to get the output waveform.
  3. Animation
    - In the **Results** toolbar, click **Animation** and choose **Player**.
    - In the **Settings** window, click **Show Frame**.

## CHAPTER 4

### RESULTS AND DISCUSSIONS

#### 4.1 Introduction

In this chapter, the results of each simulation will be discussed with different characteristics. Their output waveforms obtained by Comsol software are presented as well. The simulations can be divided into two different types, in which are that the spiral coil is moving either in vertical or horizontal direction. Furthermore, the magnetic flux density for each design is showed below to investigate how the flux density produced by the Neodymium magnet can be distributed well in a stretchable sensor.

#### 4.2 The Simulation of Spiral Coil Moving in Vertical Direction with One Fixed Permanent Magnet

In this design, one Neodymium magnet with the dimension of  $12\text{mm} \times 2\text{mm}$  is used and placed in the middle. A spiral coil with the number of turn of 5.5 is placed at the left side, and moves up and down to cut the magnetic flux. From Figure 4.1, it shows the magnetic flux density distributed by the magnet and it can tell that the area near to the magnet has stronger magnetic flux. The number of turn for spiral coil is also changed from 5.5 turns to 10 turns in order to studying how higher the output voltage can be produced.

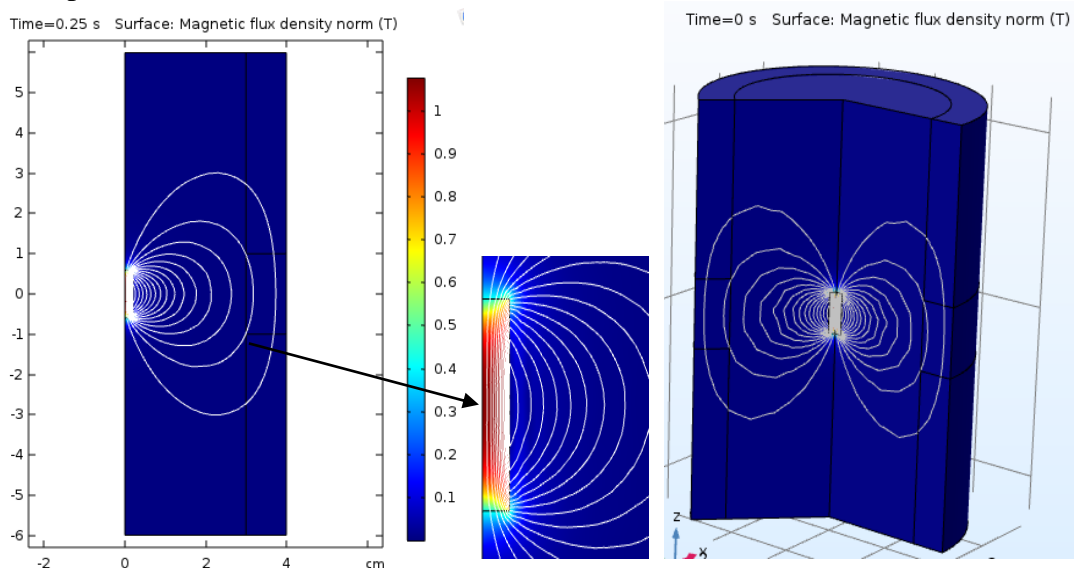


Figure 4.1: The 2D and 3D Magnetic Flux Density Norm (T in unit) Created by One Magnet where Coil moves in Vertical Direction.

Table 4.1 and Table 4.2 have showed the output waveforms that indicated the output voltage produced by the stretchable material. The distance is measured between the magnet and the spiral coil. It can be seen that when the distance is decreased, in other word, when the moving coil is closer to the magnet, the output voltage that the stretchable material can produce will much more higher which is around  $1.5 \times 10^{-3}V$ . It is because the magnetic flux around the magnet is stronger than the further area and it allows the coil to cut more flux.

In addition, by comparing Table 4.1 with Table 4.2, the number of turn for spiral coil has taken into consideration as one of the characteristic that will affect the output. The number turns is changed from 5.5 to 10, in which the length of spiral coil with 10 turns will be longer than that with 5.5 turns. It can tell that the output voltage is slightly decreased but it is supposed to be increased. The reason why it is decreased might be due to the direction of moving coil and the weak magnetic flux density. When the coil is moving in vertical direction, the cross-sectional area does not change whereas the length of the spiral coil becomes longer.

This simulation is showing that a coil inside the stretchable material is moving and thus the output voltage is considered as produced by one stretchable sensor. Therefore, the output voltage is much smaller which is among the range of  $10^{-4}V$  to  $10^{-3}V$ .

Table 4.1: The Distance between one Magnet and Spiral Coil with 5.5 Turns with the respect of Output Peak Voltage.

Magnet Size	Distance	Output Peak Voltage
$0.2cm \times 1.2cm$	$1.8cm$	$2.60 \times 10^{-4} V$
	$1.4cm$	$3.26 \times 10^{-4} V$
	$1.0cm$	$4.88 \times 10^{-4} V$
	$0.6cm$	$7.50 \times 10^{-4} V$
	$0.2cm$	$1.20 \times 10^{-3} V$
	$0cm$	$1.50 \times 10^{-3} V$

Table 4.1(Continue): The Distance between one Magnet and Spiral Coil with 5.5 Turns with the respect of Output Peak Voltage.

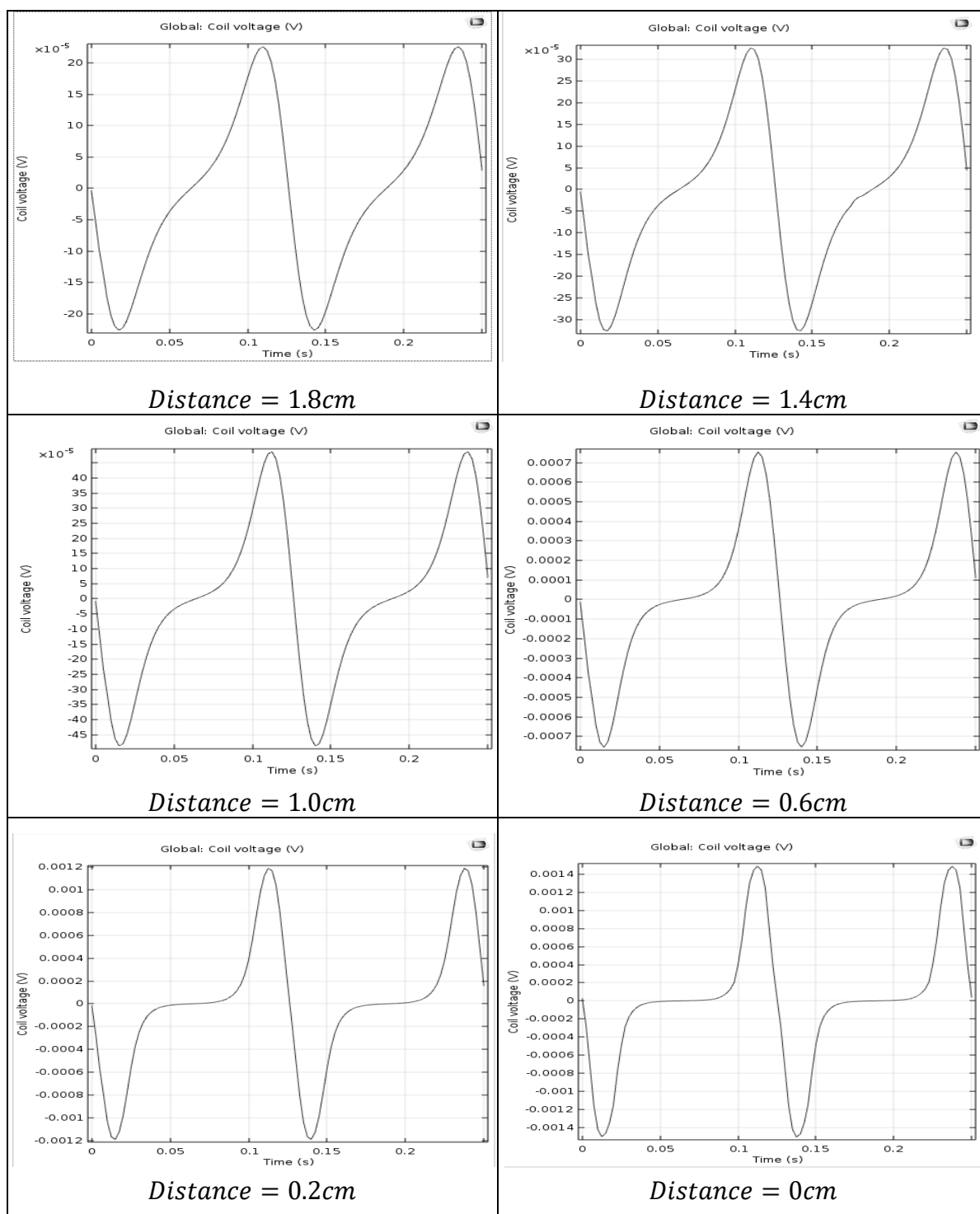
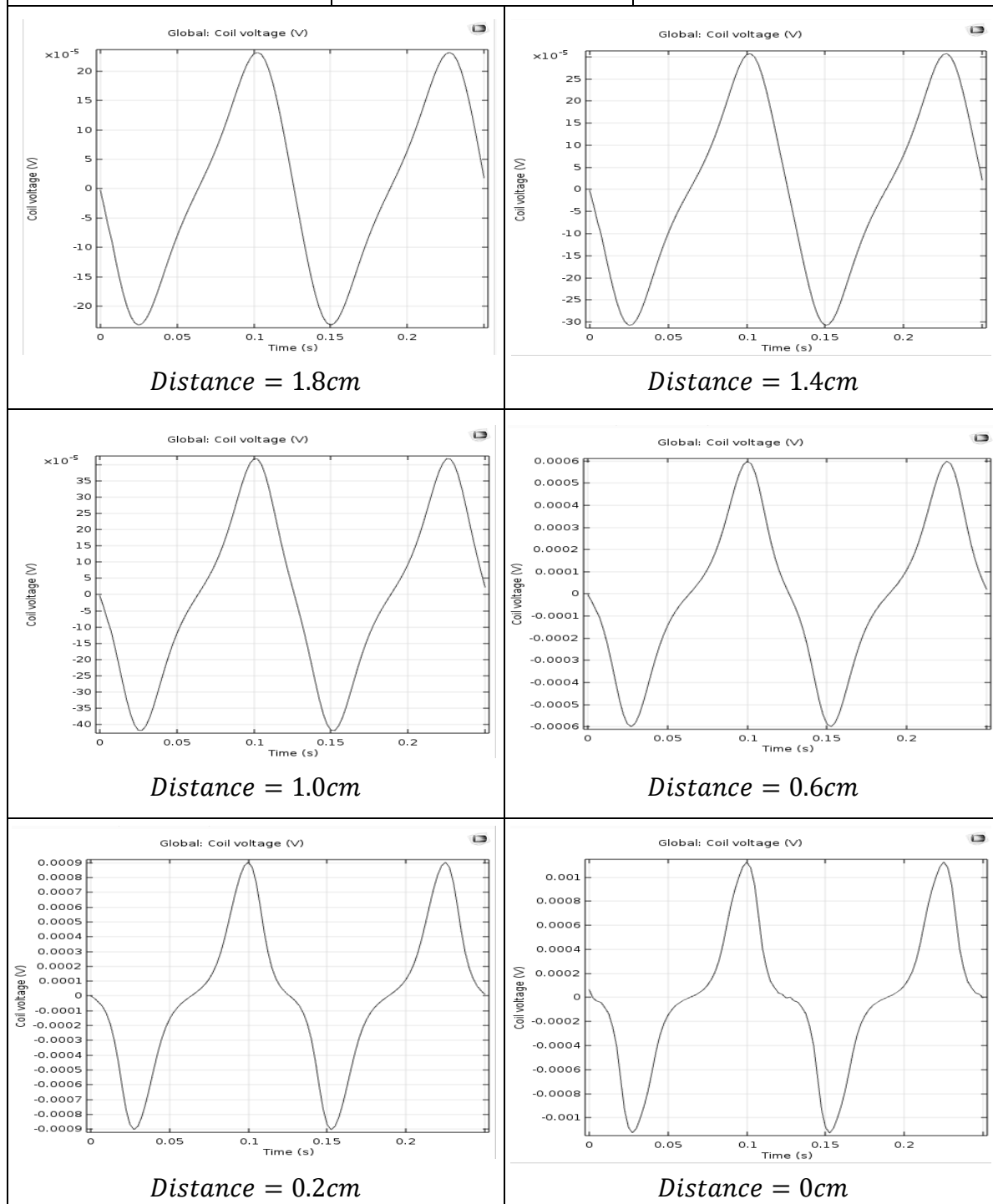


Table 4.2: The Distance between one Magnet and Spiral Coil with 10 turns with the respect of Output Peak Voltage.

Magnet Size	Distance	Output Peak Voltage
$0.2\text{cm} \times 1.2\text{cm}$	$1.8\text{cm}$	$2.32 \times 10^{-4} \text{ V}$
	$1.4\text{cm}$	$3.10 \times 10^{-4} \text{ V}$
	$1.0\text{cm}$	$4.20 \times 10^{-4} \text{ V}$
	$0.6\text{cm}$	$6.00 \times 10^{-4} \text{ V}$
	$0.2\text{cm}$	$9.00 \times 10^{-4} \text{ V}$
	$0\text{cm}$	$1.10 \times 10^{-3} \text{ V}$



### 4.3 The Simulation of Spiral Coil Moving in Vertical Direction with Two Fixed Permanent Magnets

The simulations are formed by two Neodymium magnets and a spiral coil with the number of turns of 5.5 and 10, respectively. The spiral coil will be set to move in vertical direction as well. When the coil is moving in vertical direction, it will cut the magnetic flux created by the magnets and thus produces electricity.

Figure 4.2 has indicated the magnetic flux density formed by the Neodymium magnets. It is observed that there have some magnetic fluxes between two magnets connecting together and these two magnets are supposed to be attracted instead of being appealed. Table 4.3 and Table 4.4 show the result of peak output voltage when the distance between the magnets and spiral coil is getting smaller.

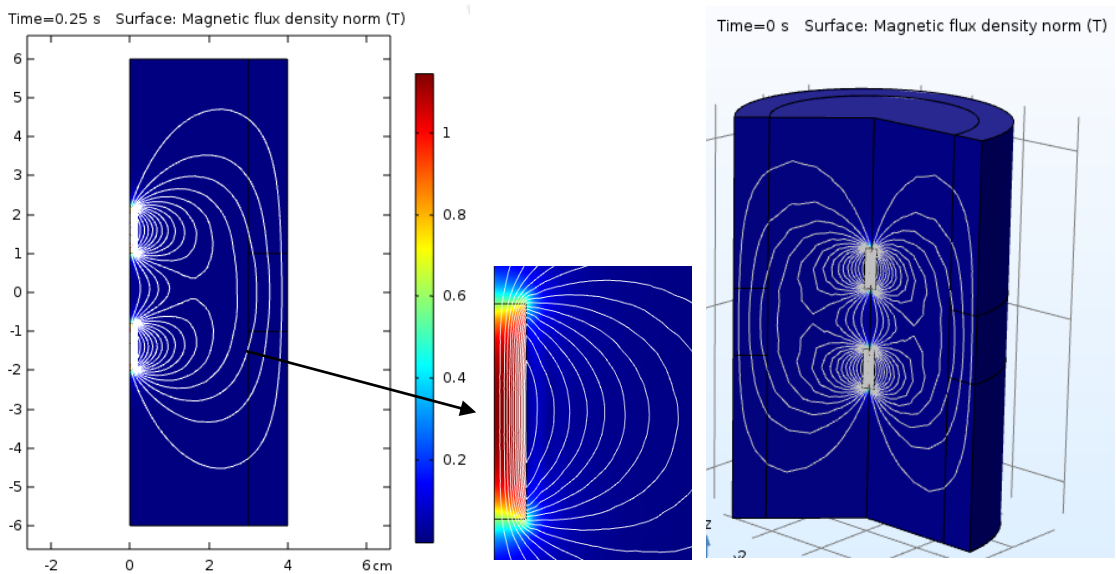


Figure 4.2: The 2D and 3D Magnetic Flux Density Norm (T in unit) Created by Two Magnets where Coil moves in Vertical Direction.

According to Table 4.3 and Table 4.4, the output voltage is getting higher when the distance between Neodymium magnets and spiral coil becomes smaller, in which the output voltage can be produced up to  $1.4 \times 10^{-3}V$ . By considering the number of turns, the stretchable material with lower turns has higher output voltage than that with 10 turns. It is also due to the direction of moving coil.

However, the overall results also prove that the model with one magnet can produce higher output voltage than that with using two magnets. Comparing Figure 4.1 with Figure 4.2, it is seen that the magnetic flux density distributed by two magnets is stronger than the one distributed by one magnet. It could be because of the spiral coil is placed and moved in vertical way, and it is parallel with the

magnetic flux, so that the second model using two magnets will produce lesser voltage.

Table 4.3: The Distance between two Magnets and Spiral Coil with 5.5 turns with the respect of Output Peak Voltage.

Magnet Size	Distance	Output Peak Voltage
<i>0.2cm × 1.2cm</i>	<i>1.8cm</i>	$1.42 \times 10^{-4} V$
	<i>1.4cm</i>	$2.00 \times 10^{-4} V$
	<i>1.0cm</i>	$2.93 \times 10^{-4} V$
	<i>0.6cm</i>	$5.00 \times 10^{-4} V$
	<i>0.2cm</i>	$1.10 \times 10^{-3} V$
	<i>0cm</i>	$1.40 \times 10^{-3} V$

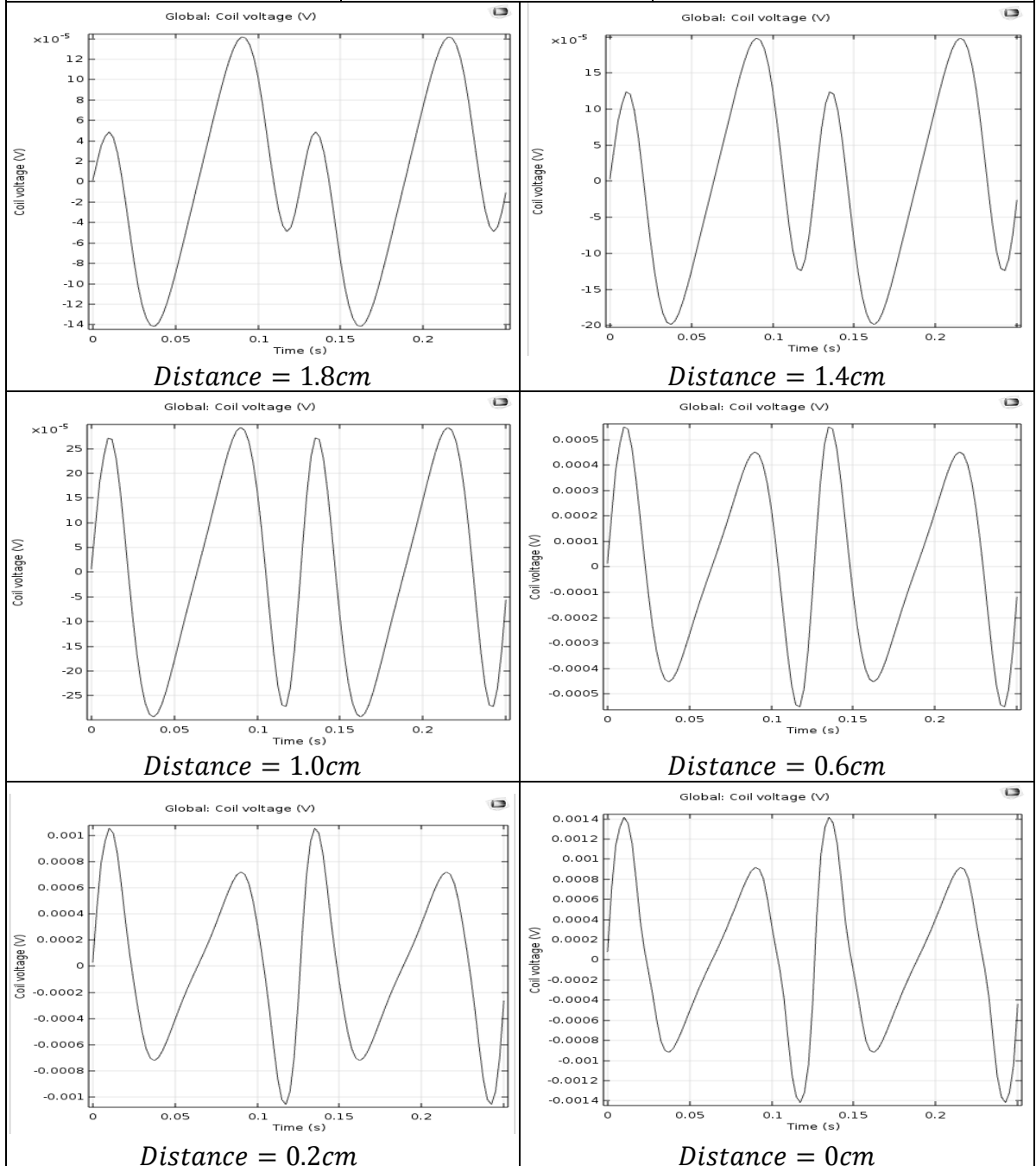
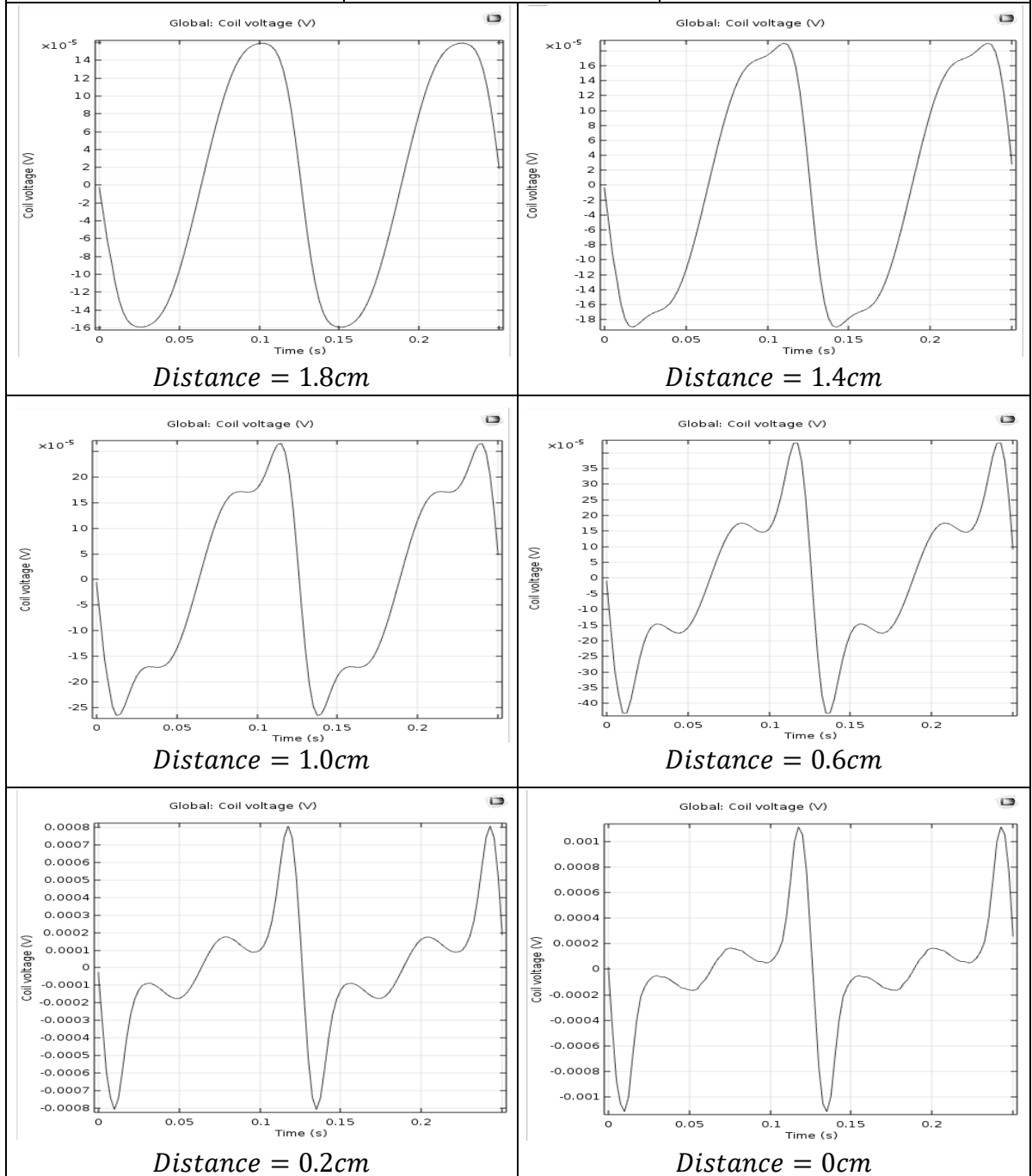


Table 4.4: The Distance between two Magnets and Spiral Coil with 10 Turns with the respect of Output Peak Voltage.

Magnet Size	Distance	Output Peak Voltage
<i>0.2cm × 1.2cm</i>	<i>1.8cm</i>	$1.60 \times 10^{-4} V$
	<i>1.4cm</i>	$1.90 \times 10^{-4} V$
	<i>1.0cm</i>	$2.66 \times 10^{-4} V$
	<i>0.6cm</i>	$4.31 \times 10^{-4} V$
	<i>0.2cm</i>	$8.10 \times 10^{-4} V$
	<i>0cm</i>	$1.10 \times 10^{-3} V$



#### 4.4 The Simulation of Spiral Coil Moving in Horizontal Direction with Two Fixed Permanent Magnets

In this part, two Neodymium magnets with the dimension of  $12\text{mm} \times 2\text{mm}$  are used and the spiral coil will be set to move in horizontal direction, in which the design can be referred to Figure 4.3 with the magnetic flux density. This simulation is actually similar to the experimental setup and the prescribed deformation is assumed as the stress applied on the spiral coil so that it will move forth and back in horizontal way. Different prescribed deformations are assumed as different stress to be applied as shown in Table 4.5 and Table 4.6 with the respect of the output waveform.

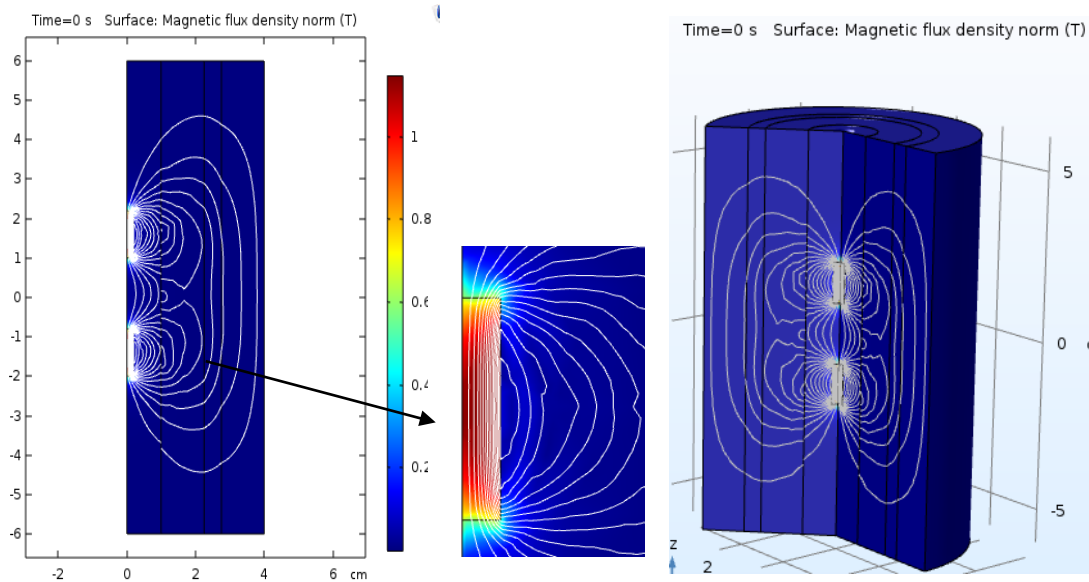


Figure 4.3: The 2D and 3D Magnetic Flux Density Norm (T in unit) Created by Two Magnets where Coil moves in Horizontal Direction.

According to Table 4.5, when the prescribed deformation or applied stress is larger, in which means that the spiral coil moves closer to the magnets, the output voltage will be increased from  $3.2 \times 10^{-6}\text{V}$  to  $9.65 \times 10^{-6}\text{V}$ . The differences for Table 4.5 and Table 4.6 are the distance between magnets and stretchable material and the thickness of stretchable material which the design shown in Table 4.6 uses thinner stretchable material. Thinner stretchable material will be more sensitive and produces higher voltage while passing through the magnetic flux. For example the same prescribed deformation of  $0.2[\text{mm}] * \sin(2 * \pi * f_0 * t)$ , the output voltage is obvious to be observed that it increases from  $6.4 \times 10^{-6}\text{V}$  to  $1.12 \times 10^{-5}\text{V}$  when the thickness of stretchable material is smaller.

Table 4.5: The Output Waveform when the Distance between Magnets and Stretchable Material is 0.8cm with the respect of Prescribed Deformation.

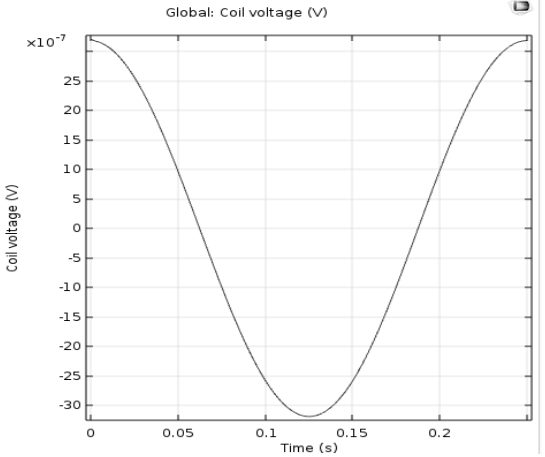
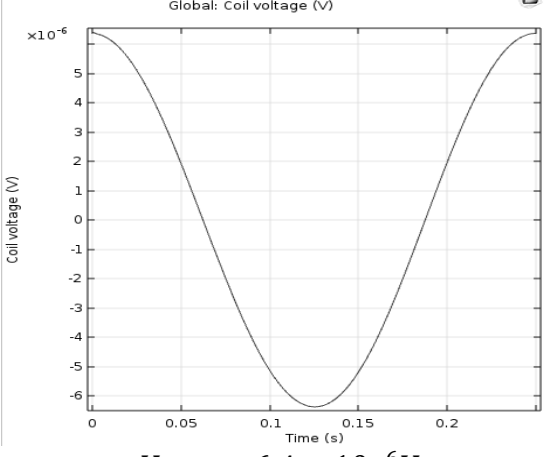
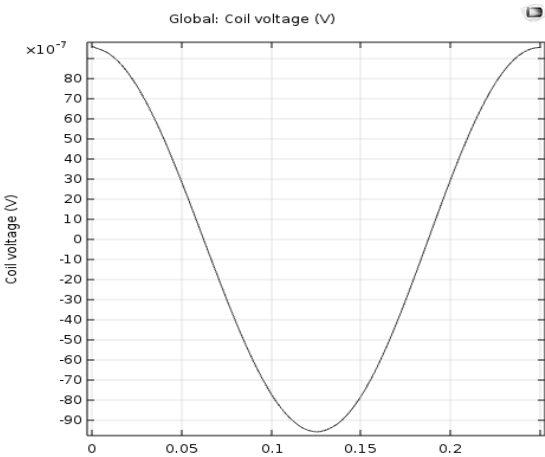
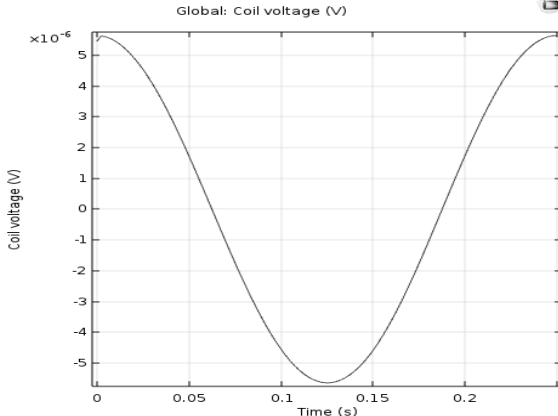
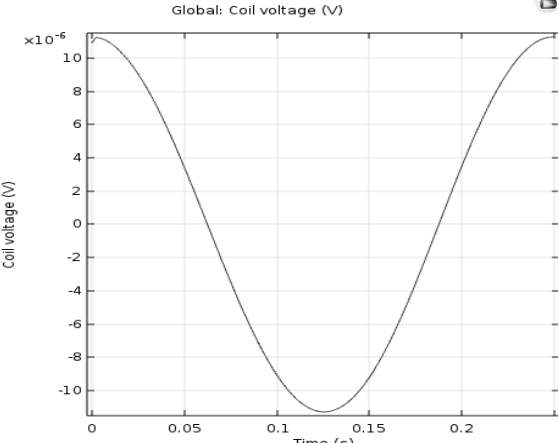
Prescribed Deformation	Output Waveform
$0.1[\text{mm}] * \sin(2 * \pi * f_0 * t)$	 <p style="text-align: center;"><math>V_{Peak} = 3.2 \times 10^{-6}V</math></p>
$0.2[\text{mm}] * \sin(2 * \pi * f_0 * t)$	 <p style="text-align: center;"><math>V_{Peak} = 6.4 \times 10^{-6}V</math></p>
$0.3[\text{mm}] * \sin(2 * \pi * f_0 * t)$	 <p style="text-align: center;"><math>V_{Peak} = 9.65 \times 10^{-6}V</math></p>

Table 4.6: The Output Waveform when the Distance between Magnets and Stretchable Material is 0.3cm with the respect of Prescribed Deformation.

Prescribed Deformation	Output Waveform
$0.1[\text{mm}]\cdot\sin(2\cdot\pi\cdot f_0\cdot t)$	 <p style="text-align: center;"><math>V_{Peak} = 5.65 \times 10^{-6}V</math></p>
$0.2[\text{mm}]\cdot\sin(2\cdot\pi\cdot f_0\cdot t)$	 <p style="text-align: center;"><math>V_{Peak} = 1.12 \times 10^{-5}V</math></p>

#### 4.5 Summary

In this section, a sequence of the simulations is investigated based on the distance between Neodymium magnet and stretchable material, the number of turns of spiral coil, and the dimension and quantity of the magnet. Although the output voltage is proved that it is increased with the smaller distance between magnet and stretchable material due to passing through the magnetic flux, the overall result is not ideal and some improvement is needed such as the size of the magnet and the better placement for magnet and the stretchable sensor so that it can produce better output voltage.

## CHAPTER 5

### CONCLUSIONS AND RECOMMENDATIONS

#### 5.1 Conclusions

In conclusion, this research is to apply electromagnetic energy harvesting method on raindrop harvester to produce electricity via vibration. In experiment, water droplets are assumed as the raindrops falling on the surface of stretchable material and induce vibration to cut through the magnetic flux distributed by the Neodymium magnets. A brief explanation about experimental setup has been illustrated in Figure 3.1. However, this research will more concentrate on the simulation instead of hardware testing which can refer to Figure 3.2 and Figure 3.3. The 2D axial symmetrical models are drawn using Comsol multiphysics 5.3a and a sequence of output waveform is obtained as shown in Chapter 4 result part.

In the simulation, Neodymium magnets are fixed and the spiral coil is moved like there is some vibration on the coil. These simulations are separated into two parts which the coil is moved either in vertical or horizontal direction. The simulated results are closer to each other no matter which direction the coil moves. The overall output voltage showed in Figure 5.1 and 5.2 is significantly low which is around  $10^{-3}V$  to  $10^{-6}V$ . From the result, it also can be observed that the nearer the spiral coil to the magnets, the higher output voltage can be produced as more magnetic flux are passed through. Furthermore, the size of the magnet is too small that the magnetic field is not strong enough. Thus, larger magnet which is almost the size of the spiral coil is suggested to be used in order to produce high electricity.

Last but not least, the simulation in section 4.4 which the spiral coil is moved in horizontal direction showed that the higher output voltage can be produced when larger force is applied on the sensor. The dimension and thickness of the stretchable sensor is also one of the characteristics needed to take into consideration. The thinner the sensor is, the higher the output voltage can be induced. Since the low power can be obtained from the sensor and also the limited sources for energy harvester, energy storage is essential to be applied for later use.

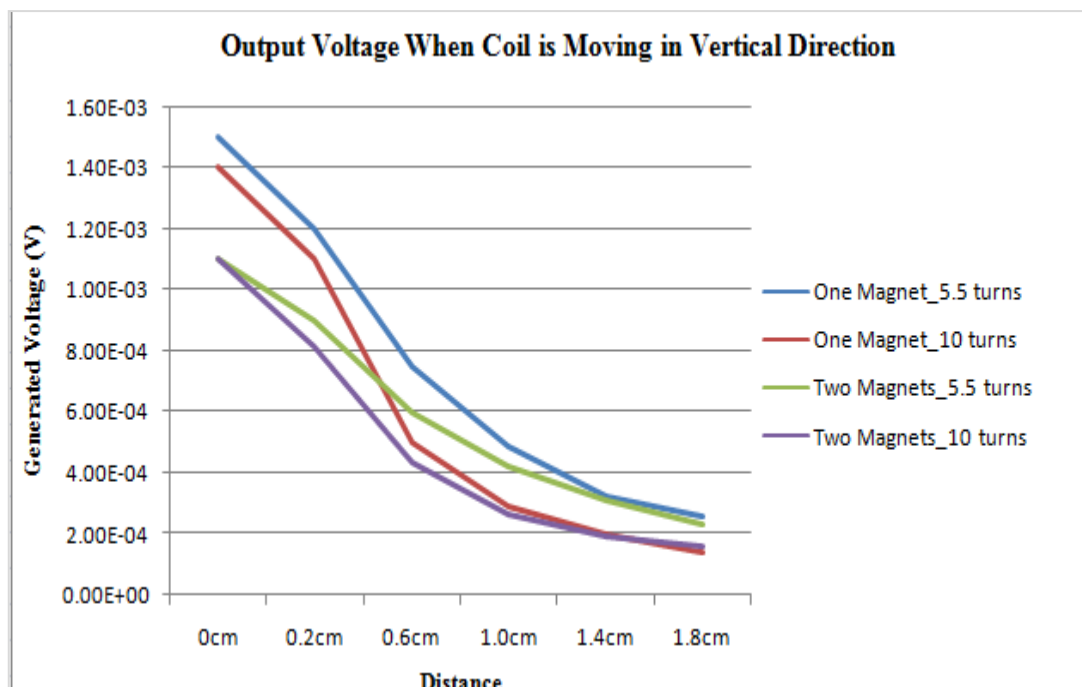


Figure 5.1: The Comparison of Output Voltage for Each Characteristic When Coil is Moving in Vertical Direction.

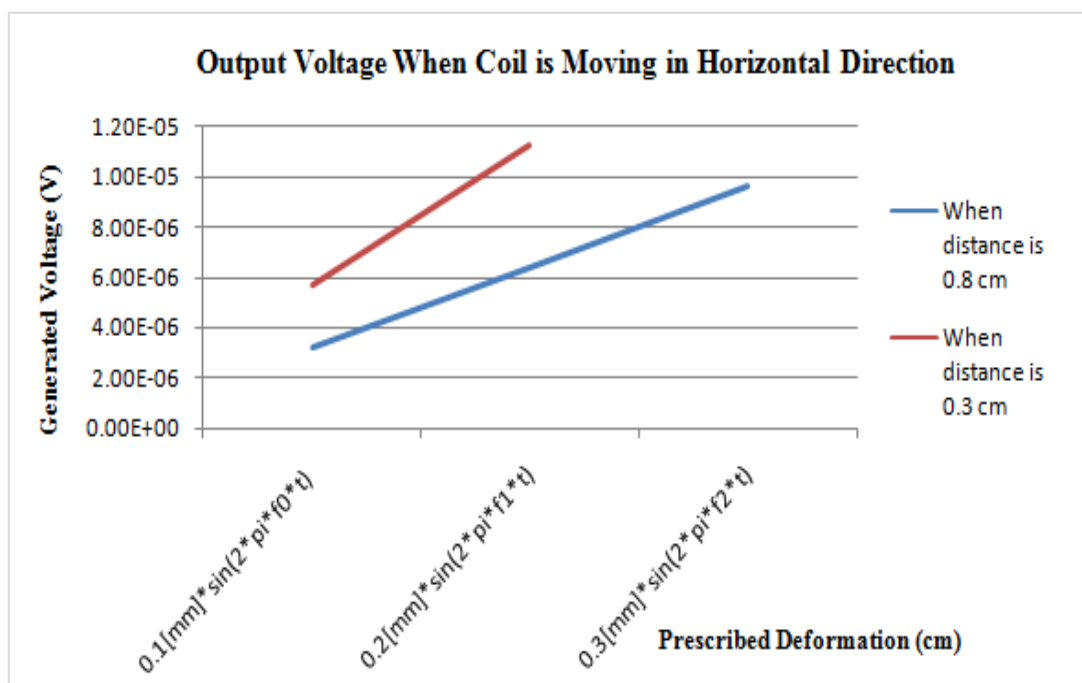


Figure 5.2: The Comparison of Output Voltage for Each Characteristic When Coil is Moving in Horizontal Direction.

## 5.2 Recommendations for future work

From this project, it can be noticed that the simulated output voltage generated by the raindrop energy harvester is too small and it is difficult to power a devices. However, when lot of energy harvesters are made together, it can produce large amount electricity. There still have some improvement needed for the design in future.

In order to managing and storing the extra electricity, rectifying circuit is suggested to store the harvested energy for later use when there is no power supplied to the electronic devices. There have lot of circuits shown in Figure 5.1, in which they are Half-bridge circuit, Full-bridge circuit, voltage doubler circuit, Cockcroft Walton Cascade Voltage Doubler circuit (CWCVD), Karthaus Fisher Cascade Voltage Doubler circuit (KFCVD). According to simulations done by Abidin, N. A. et al., voltage doubler circuit is the one more effective, KFCVD is the best to reduce voltage ripple. However, in the realistic systems, Full-bridge rectifying circuit has shown the best performance compared with the simulation (Acciari et al., 2018).

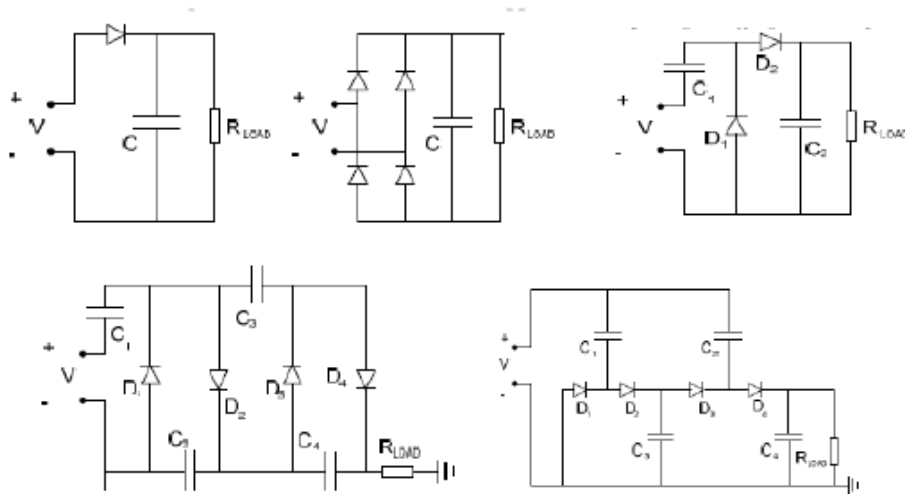


Figure 5.3: Different Types of Rectifying Circuit for Energy Storage (Acciari et al., 2018).

## REFERENCES

- Acciari, G. et al., 2018. Experimental Investigation on Different Rainfall Energy Harvesting Structures.
- Aziz, P.D.A., Wahid, S.S.A., Arief, Y.Z. and Aziz, N.A., 2016. Evaluation of Solar Energy Potential in Malaysia. *Research Article*, 9(2), pp.35–43.
- Mahammad A Hannan, S. M. (2014). Energy harvesting for the implantable biomedical devices: issues and challenges.
- Chossat, J.B., Park, Y.L., Wood, R.J. and Duchaine, V., 2013. A soft strain sensor based on ionic and metal liquids. *IEEE Sensors Journal*, 13(9), pp.3405–3414.
- Fowler, A.G., Moheimani, S.O.R. and Behrens, S., 2013. A 3-DOF SOI MEMS ultrasonic energy harvester for implanted devices. *Journal of Physics: Conference Series*, 476.
- Hannan, M. a, Mutashar, S., Samad, S. a and Hussain, A., 2014. Energy harvesting for the implantable biomedical devices: issues and challenges. *Biomedical engineering online*, 13(1), p.79.
- HR, N., 2015. Power Generation Using Piezoelectric Material. *Journal of Material Science & Engineering*, 4(3), pp.1–4.
- Jin, S.W. et al., 2015. Stretchable Loudspeaker using Liquid Metal Microchannel. *Scientific Reports*, 5(1), p.11695.
- Knier, G., 2008. How do Photovoltaics Work? - NASA Science. , 8.
- Liu, T., Sen, P. and Kim, C.J., 2012. Characterization of nontoxic liquid-metal alloy galinstan for applications in microdevices. *Journal of Microelectromechanical Systems*, 21(2), pp.443–450.
- Magdy, M.M. et al., 2014. Human Motion Spectrum - Based 2 - DOF Energy Harvesting Device : Design Methodology and Experimental Validation. *Procedia Engineering*, 87, pp.1218–1221.
- Mitcheson, P.D. et al., 2008. Energy harvesting from human and machine motion for wireless electronic devices. *Proceedings of the IEEE*, 96(9), pp.1457–1486.
- Murakawa, K., Kobayashi, M., Nakamura, O. and Kawata, S., 1999. A wireless near-infrared energy system for medical implants. *IEEE Engineering in Medicine and Biology Magazine*, 18, pp.70–72.
- N.-T. Nguyen, S. A. M. Shaegh, N. Kashaninejad, and D.-T. Phan, “Design, fabrication and characterization of drug delivery systems based on lab-on-a-chip technology,” *Advanced drug delivery reviews* (2013).

- Olivo, J., Carrara, S., De Micheli, G. and Micheli, G. De, 2011. Energy Harvesting and Remote Powering for Implantable Biosensors. *IEEE Sensors Journal*, 11(7), pp.1573–1586..
- Park, Y.L., Chen, B.R. and Wood, R.J., 2012. Design and fabrication of soft artificial skin using embedded microchannels and liquid conductors. *IEEE Sensors Journal*, 12(8), pp.2711–2718.
- Phillips, W.B., Towe, B.C. and Larson, P.J., 2003. An ultrasonically-driven piezoelectric neural stimulator. *Proceedings of the 25th Annual International Conference of the IEEE Engineering in Medicine and Biology Society (IEEE Cat. No.03CH37439)*, 2, pp.1983–1986.
- Res, I.E., Kour, R. and Charif, A., 2016. Innovative Energy & Research Piezoelectric Roads : Energy Harvesting Method Using Piezoelectric Technology. *Innovative Energy & Research*, 5(1), pp.1–6.
- Sawma, C., Sawan, M. and Kassem, A., 2015. Capacitive data links intended for implantable medical devices: A survey. *2015 International Conference on Advances in Biomedical Engineering, ICABME 2015*, pp.266–269.
- Tiwana, M.I., Redmond, S.J. and Lovell, N.H., 2012. A review of tactile sensing technologies with applications in biomedical engineering. *Sensors and Actuators A: Physical*, 179, pp.17–31.
- Vogt, D.M., Park, Y.-L. and Wood, R.J., 2013. Design and Characterization of a Soft Multi-Axis Force Sensor Using Embedded Microfluidic Channels. *IEEE Sensors Journal*, 13(10), pp.4056–4064.
- Wagner, S. and Bauer, S., 2012. Materials for stretchable electronics. *MRS Bulletin*, 37(3), pp.207–213.
- Yildiz, S.K., Mutlu, R. and Alici, G., 2016. Performance quantification of strain sensors for flexible manipulators. *IEEE/ASME International Conference on Advanced Intelligent Mechatronics, AIM*, 2016–Septe, pp.584–589.